one day, this solid was filtered, washed with water, and air-dried. The XRD results for these materials are shown in Table 3 below.

Table 3. XRD Results for Phosphonium Exchanged Clays

	Phosphonium	d-spacing (Å)
a	Tetraoctyl	22.3
b	Tetraphenyl	16.5
c	Dodecyl Triphenyl	16.5
d	C16 Triphenyl	34.4
e	C16 Tributyl	21.8

3. Lower Exchanged Phosphoniums

To help reduce or eliminate an undesired lowering of the glass transition temperature (T_g), organic content of particular nanocomposites was reduced by lowering the amount initially used for the ion exchange of the natural clays. The method outlined above for ion exchange was followed, except lower amounts of the phosphonium bromide were used as shown in Table 4, below.

Table 4. XRD Results for Low Exchange C_{16} TributylPhosphonium Clays

Type of Phosphonium	Amount of Phosphonium added	d-spacing (Å)
C_{18}tributyl	1.5	21.40
C_{18}tributyl	0.75	20.08
C_{18}tributyl	0.5	17.14
C_{18}tributyl	0.25	15.41
C_{16} tributyl	1.5	21.08
C_{16} tributyl	1.0	20.03
C_{16} tributyl	0.75	19.54
C_{16} tributyl	0.5	16.66

As can be seen from Table 4, above, the d-spacing for the lower-exchanged phosphonium clays clearly decreases with lower phosphonium content. This is consistent for a clay with less organic pillaring the layers apart. Each of these materials was extruded with Ultem 1010, as shown elsewhere in this disclosure. All of them result in intercalated or exfoliated nanocomposites. That is, increased d-spacing was observed.

The lower (underexchanged) phosphoniums were made as follows: Sodium montmorillonite (100g, 0.1mol Na+) with an exchange capacity of 100 meq/100g was added to water (1 liter). This was treated in an ultrasound bath at 80C for 1 hour. Upon addition of hexadecyltributylphosphonium bromide (101.53g, mmol, 0.2 mol) dissolved in ethanol (500ml) a white precipitate formed. After stirring for 8 hours, the solid was filtered, washed with water (1 liter) and ethanol (1liter), and dried at 90C for 6 hours. The lower exchange phosphonium clays were prepared in the same manner except with lower amounts of the phosphonium salt.

See also the TEM image of Figure 10 showing tetraoctyl phosphonium exchanged Clay/Ultem nanocomposite.

Example 4-Extruded Polymer / Layered Silicate Nanocomposites

1. Polyetherimide (PEI) Nanocomposites

Several sets of extrusions were performed using Ultem 1010 polyetherimide as the polymer matrix. The use of ORMLAS synthetic clays showed no peaks in the XRD patterns, implying a complete dispersion within the polymer up to a level of at least 10%. The phosphonium-exchanged natural clays have not been completely dispersed. The use of a C_{16}triphenyl phosphonium-exchanged clays result in a decrease in d-spacing upon nanocomposition. This has been observed previously for phenyl phosphonium clays and may be a combination of intercalation and collapse of the clay layers. Conversely, the C_{16} and C_{18} tributyl phosphonium clays result in a increase in d-spacing showing classic intercalation behavior. The fully exchanged C_{18} clays do not increase the separation of the layers significantly over that of the C_{16} analogues, however they have very sharp peaks, indicating a very well ordered material. PEI nanocomposites prepared with lower organic content phosphonium clays prepared displayed an increase in d-spacing as the organic content was lowered, despite the opposite trend in the patterns for the neat clay. The phosphonium clays prepared with a lower organic content for showed comparable patterns upon extrusion with the polymer despite their original dissimilar patterns.

Table 5. Polyetherimide Nanocomposites

Clay	%	Nano XRD (Å)	Clay XRD (Å)	T_g (°C)
Neat Ultem 1010 (GE)				**218.4**
C_{16} phenyl phosphonium	5	16.5	34.4	214.9
"	7.5	16.3	"	208.1
"	10	16.8	"	206.4
C_{18} ORMLAS	2.5	No peaks	53.5	219.1
"	5	"	"	217.4
"	7.5	"	"	217.5
"	10	"	"	215.6
1x C_{18} butyl phosphonium	1			219.3
	2.5			218.9
	5	26.3 sharp	21.4	219.2
"	7.5			217.5
"	10	27.8 sharp	21.4	217.0
¾x C_{18} butyl phosphonium	5	28.9	20.1	216.3
½x C_{18} butyl phosphonium	5	33.8	17.1	214.8
¼x C_{18} butyl phosphonium	5	No Peaks	15.4	218.8
1x C_{16} butyl phosphonium	5	26.2 broad	21.0	219.0
¾x C_{16} butyl phosphonium	5	26.9 broad	19.6	218.6
½x C_{16} butyl phosphonium	5	28.4 broad	16.7	219.6

The glass transition temperatures (Tg) obtained from DSC experiments for the various nanocomposites are also shown in Table 5, above. The DSC curves for the C_{16} triphenyl phosphonium nanocomposites show a decrease in T_g with increasing clay content. Without wishing to be bound to theory, this may be due to a large amount of organic present (in the form of phosphonium) causing plasticization. Incomplete washing of the clay during the original synthesis may be one of the reasons for this extra organic present. Conversely, the C_{18} tributyl and the lower exchanged C_{16} tributyl do not show a sharp decrease in T_g resulting in lower plasticization. The C_{18} ORMLAS synthetic clay shows a distinct decrease in T_g similar to the other ORMLAS nanocomposites reported earlier. The lowering of T_g is also likely due to plasticization since the ORMLAS materials are intrinsically high in organic content.

2. Polysulfone / Polyarylsulfone Nanocomposites

XRD and DSC results for the polysulfone and polyarylsulfone nanocomposites were obtained. The use of C_{16} butyl phosphonium clay with Udel polysulfone does not show the intercalation behavior observed with the Ultem nanocomposites. The DSC shows minimal loss in T_g as with the Ultem nanocomposites. The use of C_{16} phenyl phosphonium clay with Radel polyarylsulfone shows no peaks in the XRD patterns, however, the T_g does decrease dramatically as observed before. Both the Udel and Radel nanocomposites with phosphonium clays were very brittle possibly due to decomposition of the polymer or incomplete intercalation/exfoliation. The ORMLAS clays dispersed well in Udel, however, showed low T_g values.

3. Nylon-6 Nanocomposites

Several new nanocomposites were made using ORMLAS materials as shown below for Nylon-6. See Table 6, below.

Table 6. Nylon-6 Nanocomposites

Clay	%	Nano XRD (Å)	Clay XRD (Å)	T_g (°C)	T_m (°C)
Neat Nylon-6				**57.22**	**225.48**
C_{18} ORMLAS	2.5	No peaks	53.0	None	222.07
"	5	"	"	"	224.52
"	7.5	"	"	"	223.00

4. Other Polymer Nanocomposites

Due to the excellent results in dispersing the C18 ORMLAS within Ultem, this clay was also used with various other polymers. The XRD results for nanocomposites prepared with 5% C18 ORMLAS within these polymers are shown in Table 7, below. In every case, the XRD patterns have no peaks, implying that in every polymer the individual layers of the ORMLAS are separated and disordered within the matrix. This shows the diversity of the ORMLAS materials compared to the natural clays. A typical XRD pattern of one of these nanocomposites is shown in Figure 9. The reason for the ease of dispersion of the individual layers comes from the small size of the platelets. This can be seen in the TEM pictures where the particles on the order of 50-

100nm in diameter. This is 10x smaller than the size of the platelets in natural clays that are on the order of 1 micron. This smaller size decreases the effective Van der Waal's forces between adjacent layers, allowing their separation. The use of the long chain alkyl groups in ORMLAS also yields a much higher density of the waxy organic moieties than can exist within a natural clay.

Table 7. XRD Results for Extruded Polymer / C18 ORMLAS Nanocomposites

	Clay	Polymer	d-spacing (Å)
a	C18 ORMLAS	Udel	No peaks
b	"	Vectra A950	No peaks
c	"	Vectra A950	No peaks
d	"	Nylon	No peaks
e	"	PET	No peaks
f	"	PP	No peaks
g	"	Hytrel Polyester copolymer	No peaks
h	"	Texin Polyurethane	No peaks

Additionally, use of polyphenylene sulfide (PPS), polyphthalamide (PPA), and polycarbonate (PC) did not show peaks as determined by this analysis.

Example 5 - DMA Results for Selected Nanocomposites

The DMA curves for neat Nylon-6 and a 5% C_{18} ORMLAS / Nylon-6 nanocomposite are shown in the following graph. These results show a significantly higher storage modulus before the T_g of the nanocomposite as compared to the neat polymer. Moreover, the rubber modulus after the T_g is double to triple that of the neat polymer. Interestingly, the DSC curve for the nanocomposite earlier did not show a distinct T_g. This enlightens our understanding of how a polymer will have a HDT significantly higher than its T_g. Based on the graph, a bar with a load of 1000 MPa put on a bar of Nylon would theoretically distort at about 60°C, whereas the same load put on a bar of the nanocomposite would distort at about 130°C. Thus the Nylon nanocomposite will have an enhanced use temperature over the neat resin.

Example 6- Additional Analysis

1. Transmission Electron Microscopy (TEM)

Several nanocomposites were studied for the dispersion or exfoliation of the clay within the polymer matrix. Figure 8 shows the TEM picture of a typical ORMLAS material. It is easy to see the individual stacked up layers within each clay particle. Upon extruding within Ultem, the individual silicate layers are separated throughout the polymer matrix. These individual layers are shown in the TEM of the Ultem nanocomposite with C18 ORMLAS. See Figure 9. The enlarged inset picture shows several of the layers that are still loosely aggregated, however, the large portion of layers are completely separated from each other. The TEM of tetraoctyl phosphonium exchanged clay nanocomposite is shown in Figure 10. Although the XRD of this material does not show intercalation or exfoliation, the clay is very nicely dispersed throughout the polymer. Note the difference in the size and morphology of the ORMLAS layers compared to those of the natural clay. A sepiolite / Ultem extruded nanocomposite is shown in Figure 11. This material is not a layered clay, but a rod-like silicate. Despite not having layers that can exfoliate, the material disperses evenly throughout the matrix, and has excellent orientation.

Dynamic Mechanical Analysis was performed on neat Udel (polysulfone) and a Udel / 10%C_{16} butyl phosphonium nanocomposite. The DMA curves for these two samples are shown in the graph provided in Example 5. The HDT calculated for the nanocomposite is about 179.5 compared with the literature value of 174°C for the neat polysulfone. It suggests that the modulus as well as the HDT of Udel polysulfone can be increased somewhat over the values for the neat polymer.

See also Figure 20 showing DMA curves for a) neat Udel and b) Udel nanocomposite.

Example 7- Solution Nanocomposition

A new solution route was used to prepare nanocomposites. This was done to see the high temperature extrusion could be avoided. Also, it is possible that this route may obtain a better dispersion of the various clays. This approach has potential to work very well, since the internal surface of the clays is very organophilic, especially in the case of ORMLAS. The individual silicate layers should exfoliate in solution, as the solvent acts as a surfactant, separating the layers apart.

The solution nanocomposition took place by the following procedure. The clay was initially treated in an ultrasound bath for 10-30 minutes with the appropriate solvent for the polymer ($CHCl_3$ or CH_2Cl_2 was used for Ultem, Udel, PC). This suspension was then added to a predissolved solution of the polymer. The amount of clay was varied between 5-10 mass percent of the total solids. This suspension was then stirred for one day, then cast into a beaker or petri dish. The solvent was then evaporated in air, resulting in a free standing nanocomposite film. XRD results for the solution-prepared nanocomposites are shown in Table 8, below.

The Southern Clay natural and ammonium exchanged clays (organoclays) were used initially to determine their interaction with Ultem. The Na^+ clay showed intercalation of polymer by the increase in its d-spacing in the XRD patterns. This is quite surprising considering that that clay is very hydrophilic. The clay did not disperse well in the solvent, showing a good reason why intercalation occurred, and not exfoliation. The organoclays, Cloisite 25A and 30A (from Southern clay Products) dispersed very well in the solvents and became almost completely clear. Notably, these showed no peaks in the XRD patterns and the resultant films were quite translucent. Heat treatment of these materials (to press samples for DMA) resulted degradation by the burning of the organic portion of the clay, turning the material black and brittle. Although not useful for high temperature engineering plastics, this method using natural and exchanged clays could be very promising for other polymer matrices.

When the ORMLAS materials were dispersed into the solvents, the solvents became completely clear, indicating that either the individual layers were completely exfoliated within the solvent or there was a perfect index match for the indices of refraction between the solvent and the clay. The fact that the resulting ORMLAS / Ultem nanocomposites all lost their XRD, provided further evidence for good dispersion. This may be a way to make the nanocomposites as opposed to the melt extrusion process.

The final set of clays used with Ultem is the phosphonium exchanged clays. Like the extrusion nanocomposites (*vide infra*), exfoliation does not occur with the short chain phosphoniums, but do with the long chain analogues. Also, the long chain phosphonium clays disperse very well in the organic solvents whereas those with short chains do not. The interesting observation about the phosphonium clay nanocomposites is that the resultant films were quite transparent, and were substantially less brittle than those prepared with ORMLAS. This may help by giving an impact modifying effect for the material that is lacking with the ORMLAS as described later in the DMA testing section. The C16/phenyl phosphonium Ultem nanocomposite was scaled up and extruded as shown later in the extruded nanocomposite section.

Udel /ORMLAS nanocomposites behaved similarly to those with Ultem. Good dispersion or exfoliation occurred in these samples. The phosphonium-exchanged clays, however, did not disperse at all within the Udel.

The polycarbonate (PC) had some promising effect with the clay including ORMLAS. The clay could be intercalated or exfoliated within PC, however, the resultant material was very crystalline. DSC experiments run on these nanocomposites showed that PC lost its glass transition temperature (T_g) indicating that it was not amorphous anymore. Attempts to thermally compression mold these nanocomposites failed as the polymer was not easily processed. The samples were very brittle and did not hold together well.

Table 8. XRD Results from Solution Nanocomposition

Clay	Polymer	Clay d-spacing (Å)	Nano d-spacing (Å)	Indication
Na^+ Cloisite (Southern Clay)	Ultem		39.0	Intercalation
Cloisite 30A (organoclay)	Ultem	19.0	No peaks	Dispersion
Cloisite 25A (organoclay)	Ultem	19.0	No peaks	Dispersion
C12/phenyl phosphonium	Ultem	16.5	17.6	Intercalation
C16/phenyl phosphonium	Ultem	34.4	35.0(small)	Incomplete dispersion
C16/butyl phosphonium	Ultem	21.8	No peaks	Dispersion
C8 ORMLAS	Ultem	27.0	No peaks	Dispersion
C8 ORMLAS	Ultem	25.1	No peaks	Dispersion
C12 ORMLAS	Ultem	37.5	No peaks	Dispersion
C18 ORMLAS	Ultem	53.5	No peaks	Dispersion
C18 ORMLAS	Udel	53.5	No peaks	Dispersion
C16/butyl phosphonium	Udel	21.8	20.4	No change
Cloisite 25A	PC	19.0	29.5	Intercalation
C18 ORMLAS	PC	53.5	No peaks	Dispersion

Example 8A Thermogravimetric / Infrared Spectroscopy / Mass Spectroscopy Analyses

The thermal stability study of various clay samples was analyzed as follows. TGA with concurrent IR and MS analyses has been able to determine the relative thermal stability of various organically modified clays and the identity of the combusted organics from these materials. Many new ammonium exchanged montmorillonite samples have been analyzed. The ammonium exchanged clays show similar thermal stability (onset of decomposition between 200-275°C) to those reported previously. These ammonium clays decompose far below the processing temperature (340-360 °C) of the engineering resins (polyimide, polysulfone).

TGA with concurrent IR and MS analyses was carried out to determine the relative thermal stability of various organically modified clays and the identity of the

combusted organics from these materials. The thermal stability in this experiment mimiced the conditions that these materials will face during extrusion. The parameters evaluated regarding the thermal stability of various clays are:

A. Effect of the type of clay (provided by Southern Clay Products)
   1. Montmorillonite (CEC 95 meq)
   2. Hectorite (CEC 75 meq)
   3. Sepiolite (CEC 20 meq)

This experiment show the relative stability of the organics within the various types of clay. Sepiolite, for example, is a rod-like silicate with channels as opposed to the plate-like layers of montmorillonite and hectorite. Also, we will be able to see the effect of exchange capacity.

B. Effect of Chain length
i.e., C_6, C_8, C_{12}, C_{18} alkyl ammoniums

The effect of the chain length on thermal stability was examined. If N-C bond is the weakest, we may see no effect of chain length. The longer chains, however, may prevent (or postpone) oxidation.

C. Effect of Substitution
i.e., Mono *vs* Disubstituted ammoniums

D. Effect of Saturation
i.e., Saturated and Unsaturated tallow ammoniums

E. Electronic Differences
i.e., alkyls *vs* benzyl

With the alkyl group attached directly onto the aluminosilicate layer (Si-C covalent bond) the thermal stability is expected to be substantially higher than the ion exchanged clays.

Example 8B- Thermal Stability of ORMLAS Materials

The thermal stability of ORMLAS materials is key to the creation of superior high usetemperature and high performance nanocomposite systems. Their thermal stability has been characterized using Thermo-Gravimetric Analysis. Also, the maintenance of layered structures has been ascertained up to temperatures of 350°C using XRD analyses after a series of heat treatment runs under nitrogen and air atmospheres. Our objective was to ensure that the layered structures are maintained at temperatures used for melt-processing of high use-temperature polymers.

A. Thermo-Gravimetric Analysis

Thermogravimetric Analysis (TGA) of Alumino - Dodecylsilsesquioxane under nitrogen atmosphere is shown in Figure 13. The x-axis in Figure 13 displays the time of heating, the right hand side of the y-axis displays the temperature, and the weight is displayed on the left-hand side of the y-axis. The heating schedule comprised a ramp up to 250°C at 20°C/minute, a hold at 250°C for 10 minutes, then a ramp up to 350°C at 20°C/minute, and a hold at 350°C for 10 minutes. The heating schedule was generated to effectively simulate the heat conditions during the nanocomposite fabrication.

The Alumino-Dodecylsilsesquioxane powder was dried only to about 75°C before the TGA. At this stage it contains a lot of ethanol (solvent) and water which are evolved as during the initial stages of the heating. There is a weight loss of only about 2% during the 10-minute hold at 250°C, and only about 4% additional weight loss during the 10-minute hold at 350°C. Alumino-Dodecylsilsesquioxane ORMLAS material displayed good thermal stability in the temperature range of up to 350°C under inert atmospheres, with a total weight loss of only about 11%. Most of the weight loss can be accounted for by the loss of water and solvent, with very little degradation of the organic (dodecyl) groups attached to the silicon atoms. These ORMLAS materials were therefore expected to retain their layered structure under these conditions.

B. Effect of Heat on the Layered Structure of ORMLAS Materials

The effect of heat on the ordered layered structure of the ORMLAS materials has been investigated by obtaining the X-ray Diffraction patterns of Alumino-Dodecylsilsesquioxane powder after a series of controlled heat treatments. The TGA provided clear evidence that these materials sustain heat treatment up to 350°C under inert atmosphere without damage to the organic chains. Also, the retention of the Si-C bonds at these temperatures is well-documented in the literature. An objective in these experiments was to find out whether the layered structure of the ORMLAS material is maintained at the thermal conditions used for direct melt processing of the nanocomposites with high performance polymer matrices. As in the design of the heating schedule for the TGA, this series of heat treatments was designed to simulate the thermal conditions in the extruder during nanocomposite fabrication.

The powders were placed in alumina crucibles, and were heated to various temperatures under nitrogen or under air. XRD patterns of the powders were then obtained, and are shown in Figure 14A-G). The layered structure of the ORMLAS material, viz., Altunino - Dodecylsilsesquioxane, shows excellent thermal stability up to 350°C under inert as well as air atmospheres. The XRD pattern of Alumino – Dodecylsilsesquioxane powder obtained after drying in air at 75°C is shown in Figure 14A. A sharp peak indicating a d-spacing of 3.75 nm is evident in the figure, along with three more rational orders of the basal reflection. This peak gets more intense after heat treatment at 150°C for 10 minutes limier nitrogen, with the d-spacing slightly reduced down to 3.55 nm (Figure 14B). A sharp intense peak with a d-spacing of 3.29 nm is obtained after heat treatment at 200°C for 10 minutes under nitrogen (Fig. 14C). Sharp XRD peaks showing the retention of the layered structure with heat treatment at 250°C and 350°C under nitrogen and air atmospheres are shown in Figure 14D-G.

One trend evident from these patterns is a reduction in the d-spacings of layers with increasing degree of heat treatment.

This is shown in the following Table 9:

Temp. of Heat Treatment (°C)	d-spacing (nm)
Dried Powder	3.75
150°C - 10 min - N_2	3.55
200°C - 10 min - N_2	3.29
250°C - 10 min - N_2	2.94
250°C - 10 min - Air	2.65
350°C - 10 min - N_2	2.60
350°C - 10 min - Air	2.55

Nevertheless, the layered structure is retained. A computer simulation of the minimum breaking. Hence a good coverage of the silicate layers by the organic groups is obtained.energy configuration of the dodecyl chains within the layers has also been performed. It predicts that full surface coverage of the silicate layers by the organic (dodecyl) groups is obtained with only 56% of the Si-C bonds in place. Sol-gel processing of the ORMLAS materials protects the Si-C bonds.

C. Thermal stability of clays

TGA with concurrent IR and MS analyses will be able to determine the relative thermal stability of various organically modified clays and the identity of the combusted organics from these materials. The thermal stability in this experiment will hopefully mimic the conditions under which these materials will undergo during extrusion conditions. These experiments were all performed in flowing high purity nitrogen or oxygen. The TGA/DTA curves for several representative samples, an ammonium exchanged montmorillonite, a phosphonium exchanged montmorillonite, and an synthetic ORMLAS, are shown in Figure 2. The first exothermic peak in the DTA pattern and concurrent mass loss in the TGA curve listed in Table 10, below correspond to the combustion of the organic moiety within the layers. The onset of mass loss is also noted, although the IR spectra run in parallel indicate that minimal organic material is lost from the samples until the endothermic peak noted.

The first experiment was to compare the relative thermal stability of various natural clays. This was done with three clays, (a) montmorillonite, (b) hectorite, and (c) sepiolite exchanged with dihydrogenated, dimethyl tallow ammonium chloride. The sepiolite appears to have a substantially higher thermal stability than montmorillonite and hectorite, however, the onset of decomposition occurs much earlier. It should be noted that sepiolite is not a layered silicate or clay, but a rod-like silicate, and its exchange sites are likely in pores rather than between layers. Thus, intercalation / exfoliation of a polymer or other organic between the layers is not possible with this structure.

A comparison of the thermal stability of a monoalkyl and dialkyl substituted ammonium shows that the doubly substituted is more stable. This is exhibited between the decomposition of (d) monohydrotallow and (a) dihydrotallow exchanged montmorillonite. Although the onset of decomposition is similar between the two, the peak of decomposition is more that 50°C higher in the disubstituted analogue. The electron donating ability of the alkyl chains stabilizes the positive charge on the N core. Thus even more alkyl groups should deter decomposition of the organic moiety.

THE REST OF THIS PAGE IS LEFT BLANK INTENTIONALLY

Table 10. Thermal Stability of Various Clays by TGA/DTA Analyses

	Clay	Organic	Onset of Decomp (°C)- N_2	Peak Decomp (°C)- N_2	Onset of Decomp (°C)-O_2	Peak Decomp (°C)- O_2
a	Montmorillonite	Dihydrotallow dimethyl ammonium	230	308		
b	Hectorite	Dihydrotallow dimethyl ammonium	250	320		
c	Sepiolite	Dihydrotallow dimethyl ammonium	275	410		
d	Montmorillonite	Hydrotallow trimethyl ammonium	210	254		
e	Montmorillonite	Octadecyl trimethyl ammonium	250	265		
f	Montmorillonite	Coco trimethyl ammonium	220	258		
g	Montmorillonite	Dodecyl trimethyl ammonium	210	255		
h	Montmorillonite	Dodecyl triphenyl phosphonium	300	328		
i	Montmorillonite	Tetraoctyl phosphonium	320	469		
j	Montmorillonite	Tetraphenyl phosphonium	340	389		
k	C8 ORMLAS	Octyl	350	517		
l	C12 ORMLAS	Dodecyl	320	521	190	230
m	C18 ORMLAS	Octadecyl	400	509	192	238
n	C16 ORMLAS	Hexadecyl			190	240
o	Phenyl ORMLAS	Phenyl			180	230
p	Phenethyl ORMLAS	Phenethyl			260	395
q	Phenethyl / C12	25% Phenethyl			205	250
r	Phenethyl / C12	50% Phenethyl			230	264
s	Phenethyl / C12	75% Phenethyl			230	392

A further interesting note is the comparison of (d) hydrotallow (mixture of C14, C16, and C18) compared with (e) octadecyl (pure C18). The stability of the pure C18 is notably higher, and also has a significantly sharper decomposition point. This is also observed, although to a lesser extent, with coco (C12, and others) and dodecyl (pure C12). The longer chain alkyl (e *vs* g) does have a small effect in increasing thermal stability.

Comparison of the thermal decomposition of the phosphonium *vs* ammonium exchanged clays shows that the phosphonium analogues (h,i,j) have significantly higher stability. See Table 10, above. This can be explained by the better ability of P than N to delocalize the positive charge. Also, the core (P^+, where the decomposition likely originates) is protected by multi-substitution. The material with the highest thermal stability is the tetraoctyl, which has four long alkyl chains protecting the core. The alkyl chains are all electron donating, a property that has been shown earlier to stabilize the positive charge, and thus prevent thermal decomposition.

The ORMLAS materials (k,l,m) have substantially higher thermal stability than do any of the natural clays. The TGA curves for these materials are very broad with a early onset point and slowly increasing mass loss. The DTA curves, however, are fairly sharp and similar for the samples tested indicating that the organics within these clays are very stable and decompose at a very precise temperature. The fact that the thermal stability of each ORMLAS is the same indicates that the material starts to decompose when the Si-C bond is broken. Thus the stability is independent of chain length. The high stability of these materials is due to the strong Si-C bonds in the structure as compared with N^+-C as in the natural clays. All of the natural clays have cationic organic moieties that are very susceptible to decomposition. The neutral surfactant that is actually covalently bonded to the silicate surface gives a critical stabilizing effect.

Each of the ORMLAS samples has an exothermic peak and a small mass loss between 180-206 °C. The IR spectra at this temperature show that the material coming off is likely not organic or at least not alkyl derived organics. Further, mass spectroscopy confirms that very little organic material is combusted below 500 °C in any ORMLAS.

Several of the ORMLAS materials were also tested for their thermal stability in an O_2 atmosphere. The decomposition for each occurs at a significantly lower

temperature than they do in N_2. It is interesting that the alkyl ORMLAS (l,m,n) all begin to decompose at about the same temperature in O_2 (about 190°C). The similar thermal stability of these materials parallels the result of the experiment obtained under N_2. The highest stability material in the series is the one prepared with (p) Phenethyl silane. Even the addition of Phenethyl silane to the reaction mixture of Dodecyl ORMLAS increases its thermal stability substantially (q,r,s).

See also Figures 18A-C showing XRD spectra for Montmorillonite ion-exchanged with various phosphonium cations.

Example 9- Nanocomposite Compounding Methods

As discussed above, silicate compositions of this invention and particularly nanocomposites can be made using conventional extuder implemtations. Such an extruder is preferably a single or twin screw extruder such as those generally known in the field. In situations in which a a twin screw extruder is used, the preferred embodiment shall make use of a co-rotating twin screw extruder as follows.

The twin co-rotating extruder shall consist of screws with 3 distinct sets of element types including: a) conveying elements, b) kneading elements, c) mixing/dispersion elements. In particular, 5-30% of the length of each screw shall consist of kneading elements; 5-15% of the length of the screw shall consist of mixing/dispersion elements; and 55-90% of the length of the screw shall consist of conveying elements.

It is often important to maintain a carefully defined pressure profile inside the extruder. This pressure profile includes high pressure in the kneading section for a short duration, layered silicate shall be added at a low pressure area after the neat resin has been melted, the mixing section shall be at lower pressure than in the kneading section, the conveyance section shall be approximately three times longer than the kneading section.

More specifically, to make the nanocomposite, the screws shall exhibit a length over diameter ratio (L/D) of between 30-35 to 1. The screw speed shall operate between 50-166 RPM.

There are generally two preferred methods of feeding the materials to be compounded into the extruder, namely by premixing the plastic resin with the nanoloyered silicate and by feeding the two separately.

In the cases in which the desired nanocomposite includes polymer blends or alloys, the polymers (two or more) may also be premixed or introduced along the length of the extruder.

For example, the polymer and the layered silicate shall be gravimetrically fed using a starve feeding methodology. Starve feeding introduces the material to be mixed using a controlled rate system. Use of starve feeding is essential to controlled mixing of the two components. The layered silicate shall be fed approximately 50% along the length of the extruder in order to allow the neat resin to reach its melting point.

One good way of feeding involves first feeding the thermoplastic resin in powder or pellet form. The extruder shall be preheated to a temperature set at 99%-110% of the melting point of the neat resin. The neat resin shall be at 99%-110% of its melting point at the point of intercalation or exfoliation. Such temperature profile shall be maintained during the mixing (compounding).

The exiting compounded (resin plus layered silicate) resin shall have a temperature of 102-110% of the melting point of the neat resin. In order to obtain compounded material with optimum properties, it is essential to extract entrapped volatiles in gaseous form within the last 10% of the length of the extruder.

The exiting compounded shall go through a mole which shall be able to impart certain geometric configuration on the thermoplastic compound. Such geometry may

be in the form of a rod, film, sheet, or other complex shapes such as blow molded or extrusion blow molded article of manufacture.

For applications in which an article of manufacture is to be made, that article exiting the extruder shall be quenched to a temperature of 10-100°C using liquid (such as water) or gaseous material (such as nitrogen or air).

A. Al n-Dodecylsilsesquioxane and Nylon 6

Nylon-6 has been used as the benchmark polymer matrix due to the vast amount of data avails le on Nylon-nanocomposites. The nanocomposites were fabricated via solvent free Direct melt processing using a twin-screw extruder. The extruder was maintained at a temperature high enough to ensure the presence of a polymer melt (235'C for Nylon-6). A residence time of 5-10 minutes at the melt temperature was used. A purge of nitrogen was maintained during the heating. The extruder was cleaned between the runs by passing pure polymer through.

a) ORMLAS

X-ray diffraction pattern of the nanocomposites made using 5 wt % of Al n-Dodecyl stlsesquioxane with Nylon-6 does not show any crystalline features which is indicative of a good dispersion of the ORMLAS layers in the polymer matrix. Further evaluation of the effect of extrusion on the layered structures of the ORMLAS materials was done by obtaining XRD patterns of the powder mixtures of Nylon-6 with the ORMLAS materials before and after extrusion. Figures 15A-C show the patterns of mixtures of Nylon-6 powder with 5 wt.% (Figure 15A) and 7 wt.% (Figure 15B) Al n-Dodecyl silsesquioxane powder before extrusions A sharp peak corresponding to a ~ 3.9 nm is evident in both patterns, and its position matches well with that of the peak in the pattern of neat Al n-Dodecyl stlsesquloxane (Figure 15A). This peak disappears after extrusion (Figure 15C). Similar trends were obtained with much higher contents (15 and 20 wt.%) of Al n Octadecyl stlsesquioxane.

The structure of the Nylon-Dodecyl ORMLAS nanocomposites was directly examined using Transmission Electron Microscopy in order to observe the state of the

ORMLAS layers within the polymer. The particular nanocomposites examined had 15 weight % Dodecyl Silsesquioxane in a Nylon matrix, and were fabricated under a nitrogen purge at 235°C with a residence time of 10 minutes in the extruder. Figure 16A-B show the TEM pictures displaying an exfoliation of the Alumino-Dodecylsilsesquioxane layers within the Nylon matrix. The bar on the bottom of the picture represents a length of 50 nm. Individual ORMLAS layers well-dispersed within the Nylon matrix are evident in the micrograph. Thus, the surface chemistry of the ORMLAS materials provides favorable interactions with the Nylon matrix. These favorable molecular interactions result in the exfoliation of the individual layers within the polymer matrix. Such control of the surface chemistry is a very desirable achievement.

The intimate molecular interactions of the ORMLAS layers levity the Nylon matrix are also indicated by the DSC (Differential Scanning Calorimetry) measurements (Figure 17A-B). Figure 17 (A) shows the DSC plots of Nylon-6 and Nylon-ORMLAS nanocomposite obtained at a heating rate of 20°C/minute. A difference of ~ 15°C in the melting temperature is evident, and was repeatedly observed. This was interpreted to be a kinetic effect of the molecularly dispersed ORMLAS layers on the flow of the polymer chains. Indeed, a slower heating rate (100°C/minute) lowers the observed peak by ~15°C (Figure 17B). This observation suggest that an extremely intimate mixture of the ORMLAS layers with the Nylon matrix is formed in the nanocomposite.

Having made synthetic layered silicate phase which provides a favorable interracial chemistry as well as a more thermally stable interface, ORMLAS and higher use-temperature resins have been combined. We have fabricated nanocomposites using Polyetherimide (Ultem 1000 and Ultem 1010) as the matrix. These polymer resins have a Heat Distortion Temperature (HDT) of about 200°C, and can be extruded at about 335-340°C. This is ideal to examine any enhancements in thermal and mechanical properties of nanocomposites in the range of 200-250°C.

B) Phosphonium Clays

The ion-exchanged clays were mixed with Nylon and with Ultem 1010 (PolyetherImide) resin, and nanocomposites were fabricated in a twin-screw micro-extruder under a purge of nitrogen. Clays containing phenyl functionalities show poor dispersion in both Nylon and in Ultem matrices - as evidenced by the XRD patterns of the extruded product (Figure 19A). Sharp remnant peaks related to the layered arrangement of the clays within the polymer clearly show that the phenyl-clays are not dispersing in the polymer matrix. This is consistent with our observations of poor dispersion of phenyl-ORMLAS materials in polymer matrices. The XRD pattern indicates a much better dispersion of the tetraoctyl-exchanged clays in the polymers (Figure 19B). By creating a favorable chemistry at the interface, Tetra-Octyl phosphonium therefore provided a success for this approach.

It will be understood that the information provided in this example can be readily modified to suit an intended result. For example it will be helpful in some situations to optimize pressure, heating and mixing profiles within a selected extruder implementation to facilitate a particular performance characteristic. Such optimization is within the skill of those and this field and will not require undue experimentation to achieve.

Example 10- High Barrier Nanocomposites

As discussed, the invention provides a variety of high gas-barrier nanocomposites. Such nanocomposites are made by one or a combination of approaches including compounding at least one suitable layered silicate phase with at least one base polymer resin such as PET, polyolefins, EVOH, ect. By adjusting the chemistry and the processing conditions, e.g., to suit an intended use, these nanofillers naturally self-assemble (i.e. stack up) through the thickness of the plastic sheet. The typical feature size of each filler platelet is approximately 1 nm (one billionth of a meter) in thickness, and 100-500 nm in length. The separation distance between each layer is preferably between 3 to 10 nm.

The nancomposites provided have several important characteristics including ultrafine feature sizes, low loading of the layered silicate phase, light weight, and

processibility via the conventional polymer processing techniques. Examples of such techniques are disclosed below and in Example 9 above. In most instances, the silicate layers of the nanocomposites do not adversely affect the impact strength or the puncture resistance of the base resin. Instead, they generate a tortuous path for the diffusing gas species, thus significantly increasing the diffusion distance through the thickness of the plastic. Accordingly, the high gas-barrier nanocomposites are highly useful and particularly enhance the barrier properties of commodity polymers.

More specific information relating to making and using the high gas-barrier nanocomposites is provided below.

A. Silicates

Several types of organically modified natural layered silicates were used. Following is a standard procedure for the ion exchange procedure of two standard organically modified clays. About 100 g of sodium montmorillonite (with 100 meq / 100g exchange capacity) was ion exchanged with (i) 49.07 g (100 mmol) of dimethyl hydrogenated tallow-2-ethylhexyl ammonium bromide, and (ii) 42.25 g (100 mmol) of methyltallow bis-2-hydroxyethyl ammonium bromide. The Na^+ montmorillonite was dispersed in 4 liters of water at 80°C with the aid of ultrasonic treatment. Upon the addition of a solution of the alkyl ammonium salt, a precipitation of a white solid was observed. After stirring for 24 hours, the solid was filtered and washed with copious water until the filtrate had a pH of 7. The solid was dried at 80°C for several hours, ground into a fine powder, and the smallest particulate was obtained through a 100 mesh sieve. The finely ground clays with an average particle size of about 1 micron were used.

As discussed earlier, this ion exchange with the organic groups gives the silicate layers an organic character, and creates favorable interactions with organic polymers. The creation of suitable interactions is one important factor in obtaining a nanoscale dispersion of the silicate layers, and in the creation of superior barrier and other mechanical and thermal properties.

B. Polymer Materials

The PET used was Tenite 12822 – obtained from Eastman Chemicals. This particular grade was selected in order to minimize crystallization and orientation in the matrix, which also affect the barrier properties. This grade of PET does not contain any nucleating agents which could promote the crystallization of PET matrix during extrusion. This allows for an isolation of the effects of the layered silicates on the barrier properties.

C. Nanocomposite Fabrication

Non-solvent based melt extrusion process was employed using a twin-screw extruder to fabricate the nanocomposites. A twin-screw extruder usually provides the necessary shear to ensure homogeneous distribution of the inorganic phase within the polymer matrix. The extruder was heated to a temperature that ensures the presence of a polymer melt.

A particular fabrication approach involves melt blending a suitable polymer resin and layered silicate, e.g., about 5 to 10% (w/w) NA^+-montmorillonite, with the remaining part as PET or a blend or an alloy thereof. The material is added to one extruder and feeding is achieved with a standard sheet die to produce the sheet stock for thermoforming the final parts. The twin-screw extruder is often preferred. The entire process, in production mode, will preferably occur in one continuous step, from melt blending / extrusion to "in-line thermoforming". That is, as the sheet is extruded, it passes over thermoforming molds where the sheet is formed before it gets a chance to cool.

In a more specific fabrication approach, the extrusion was carried out at 250°C. A series of PET-nanocomposites and pure PET samples was fabricated under precisely the same conditions. The extruder yielded nanocomposites in the shape of rods, which were then *thermoformed* into 5 cm x 5 cm films having a thickness of about 12 mils. The thermoforming was carried out at 250°C under high pressure in a press. Three films of each composition were prepared so as to obtain several sets of permeability measurements. See Example 9, above for more specific information

relating to compounding the nanocomposites using a conventional extruder implementations.

D. PET High Gas-barrier Nanocomposite

The results shown below in Tables 11 and 12 demonstrate up to 2 orders of magnitude improvement in oxygen barrier of PET at 0% relative humidity. Significantly, the permeability of the Nanocomposite#2 was below the detection limit of the equipment. Nanocomposite #2 shows a stronger effect (much lower oxygen permeability) because of its higher clay content – 10% compared to 5% clay in the case of Nanocomposite #1.

Table 11: Oxygen Permeability of PET and PET-nanocomposites at 0% RH

Oxygen Transmission (cc/100 in2.day)

Sample	1st Measurement	Repeat Measurement
Pure PET Control	0.94	0.63
PET Nanocomposite#1	0.09	0.06
PET Nanocomposite#2	<0.01	<0.01

PET= polyethylene tetraphthalate
RH= relative humidity

Due to the increased diffusion distance with the numerous nano-silicate layers in their path, the PET-nanocomposites also show a dramatic improvement in water barrier performance compared to the neat PET resin. The results of the water vapor permeability measurements are shown below in Table 12. Nanocomposites# 1 and #2 in Table 2 are the same films as the ones in Table 11. The results show up to about 20-fold reduction in water vapor permeability. These results are very promising and clearly show the tremendous effect of the nanolayers in reducing the gas permeability of the polymer.

Table 12: Water Vapor Permeability of PET and PET-nanocomposites at 90% RH

Water Vapor Transmission (gm/100 in2.day)

Sample	1st Measurement	Repeat Measurement
Pure PET Control	2.0	2.5
PET Nanocomposite#1	0.1	-
PET Nanocomposite#2	0.12	0.14

PET= polyethylene tetraphthalate
RH= relative humidity

E. Gas Permeability Measurements

The oxygen and water vapor permeability measurements for the above-mentioned films were carried out at Delmonte Laboratories (Walnut Creek, CA). A 5 cm^2 circular cross-section of the films described above was masked and used for these permeability measurements. The permeability of the nanocomposite samples was compared directly with that of the pure PET samples.

The oxygen permeability data shown above in Table 11 is especially impressive. The results indicate up to a 100-fold reduction in the oxygen permeability of PET at 0% relative humidity. In fact, the permeability of the Nanocomposite#2 was below the detection limit of the equipment. Nanocomposite #2 shows a stronger effect (much lower oxygen permeability) because of its higher clay content – 10% compared to 5% clay in the case of Nanocomposite #1.

F. X-ray Diffraction Analysis

The following is an analysis of the permeability data shown in Tables 11 and 12 in light of X-Ray Diffraction (XRD) analysis. As discussed throughout this application, XRD can provide useful information about the silicate layers within a nanocomposite.

X-ray diffraction analyses was performed on the layered silicate materials as well as on the PET nanocomposites to investigate the state of the layered silicates upon extrusion with the PET. Information about the state of the individual layers within the polymer matrix is thus obtained.

The patterns of the two organically modified layered silicate materials (clays) are shown in Figures 24A-B. The clays show a layered structure with an interlayer spacing of ~ 1.8-1.9 nm (Figure 24(a) and 24(b)). The XRD patterns of PET-nanocomposites containing 5% and 10% clay respectively are shown in Figure 24(a) and 25(b). These patterns clearly indicate that the layer spacing has increased from

1.8 nm in the pure clay to 3.2 nm in the nanocomposite. This indicates the intercalation of polymer into the interlayer spacing of the clays, and hence the formation of ordered intercalated hybrids. A sharp peak indicating ordered intercalates with a layer spacing of about 3.2 nm is evident, and is seen to get stronger for the 10%-clay nanocomposite sample (Nanocomposite sample #2 in Tables 3 and 4). Clearly, the original interlayer spacing of the neat clays (i. e., 1.8-1.9 nm) is enhanced to 3.2 nm by the intercalation of PET within the layers, therefore leading to intercalated *nano*composite structure.

G. Discussion

The model illustrated in Figure 23 and the observed increased diffusion distance of the gaseous species of the nanocomposites provided in Tables 11 and 12 is consistent with numerous nano-silicate layers in the path of the gas. For example, the permeability of water vapor undergoes a dramatic reduction in the nanocomposites compared to the neat PET resin. The results of the water vapor permeability measurements are shown below in Table 12. Nanocomposites# 1 and #2 in Table 12 are the same films as in Table 11. The results show up to about 20-fold reduction in water vapor permeability. These results are extremely promising and clearly show the tremendous effect of the nanolayers in reducing the gas permeability of the polymer.

The high gas-barrier nanocomposites of this invention can be used alone or in combination with other components in a wide spectrum of manufactured articles. Preferred articles are those in which good barrier properties are desired such as substantial exclusion of at least one solute, preferably a gas such as water vapor. As an example, an Army food tray can be made using at least one suitable high gas-barrier nanocomposite and preferably one of same to satisfy gas barrier requirements and create a superior product with a 3-year food shelf-life. Other suitable manufactured articles have already been discussed and include those adopted to enclose a gaseous, liquid, solid or semi-solid material. More specific examples include beverage containers and blister packs.

Example 11- High-Strength Hytrel Nanocomposite

As discussed in the U.S.S.N 60/139,481 provisional application, it is possible to make a wide variety of high-strength Hytrel nancomposites. One such nanocomposite composition uses 10% by weight of ORMLAS organosilicate described in the Examples above mixed with molten black Hytrel 5612 in an extrusion screw. The resulting material was about 30 mil thick and about 7.5 inches wide. Upon testing the material showed a shore durometer of about 51-52, a tensile strength of about 142 kg/cm and an elongation of about 500%, providing a higher tensile strength without appreciable loss of elongation as compared to black Hytrel 5612.

The material thus provides high strength and barrier properties without decreasing elasticity.

Example 12- Polymer Alloy Nancomposites

Polyolefin-layered silicate polymer nanocomposite materials were made along lines discussed above. The following Table 13 provides ranges and examples of total weight percentage of various components used to make the materials.

TABLE 13 - Preparation of Six Polymer Alloy Nanocomposites

[1]Total Wt % range		Ex 1	Ex 2	Ex 3	Ex 4	Ex 5	Ex 6	Ex 7
pp	40 - 99	70	75	40	40	50	66	97
pa	.4 - 54	20	20	.8	.9	37	7	.9
fgpp	.2 - 16	3	3	.2	.1	9	1	.1
oc	1 - 40	4	1	34	40	2	12	1
s.f.oc	0 - 25	3	1	25	19	2	14	1

1. pp= polyolefin; pa= polyamide; fgpp= functionalized grafted polyolefin; oc= organoclay; s.f.oc= synthetically formulated organoclay

All references disclosed in this application are incorporated herein by reference.

While the invention has been described with reference to specific embodiments, modifications and variations of the invention may be constructed without departing from the scope of the invention, which is defined in the following claims.

What is claimed is:

1. An inorganic layered silicate comprising at least one high temperature organic surfactant non-covalently attached to the silicate, wherein the surfactant comprises at least one onium salt having the following general formula:

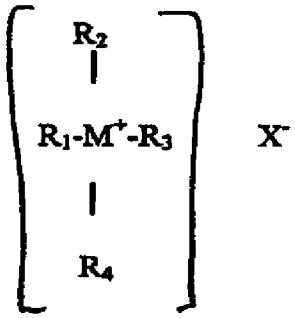

wherein M is O, S or P,

each of R1, R2, R3 and R4 is independently an optionally substituted or unsubstituted alkyl, alkenyl, alkynyl, cycloalkyl, cycloalkenyl, cycloalkynyl, aryl, alkylaryl, alkenylaryl, alkynylaryl, alkylthio, alkylsulfinyl, alkylsulfonyl, or carboxycyclic aryl group; in which each of R1, R2, R3 and R4 can be the same or different; and X^- is a counter ion.

2. The inorganic layered silicate of claim 1, wherein each of R1, R2, R3 and R4 is an octyl or phenyl group,the same or different.

3. The inorganic layered silicate of claim 2, wherein the onium salt is a substituted or unsubstituted tetraphenyl phosphonium salt.

4. The inorganic layered silicate of claim 1, wherein each of R1, R2 and R3 is a substituted or unsubstituted phenyl group and R4 is a substituted or unsubstituted alkyl group having between from about 16 to about 20 carbon atoms.

5. The inorganic layered silicate of claim 1, wherein each of R1, R2 and R3 is a butyl and R4 is a substituted or unsubstituted alkyl group having about 16 carbon atoms..

6. An inorganic layered silicate comprising at least one high temperature organic surfactant non-covalently attached to the silicate, wherein the surfactant comprises at least one onium salt and the moles of the surfactant is less than the moles of the silicate.

7. The inorganic layered silicate of claim 6, wherein the onium salt has the following general formula:

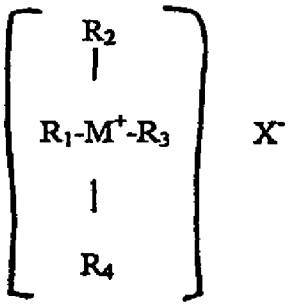

wherein M is N, O, S or P,

each of R1, R2, R3 and R4 is independently an optionally substituted or unsubstituted alkyl, alkenyl, alkynyl, cycloalkyl, cycloalkenyl, cycloalkynyl, aryl, alkylaryl, alkenylaryl, alkynylaryl, alkylthio, alkylsulfinyl, alkylsulfonyl, or carboxycyclic aryl group; in which each of R1, R2, R3 and R4 can be the same or different; and X^- is a counter ion.

8. The inorganic layered silicate of claim 7, wherein said at least one onium salt comprises at least one phosphonium salt.

9. The inorganic layered silicate of claim 8, wherein the ratio of the moles of the onium salt to the moles of the silicate is between from about 0.1 to at least about 10.

10. The inorganic layered silicate of claim 9, wherein the ratio of the moles of the onium salt to the moles of the silicate is between from about 0.25 to about 1.

11. The inorganic layered silicate of claim 10, wherein the ratio of the moles of the onium salt to the moles of the silicate is between from about 0.1 to less than 1.

12. The inorganic layered silicate of claim 11, wherein the ratio of the moles of the onium salt to the moles of the silicate is between from about 0.25 to about 0.5.

13. The inorganic layered silicate of claim 1 or 6, wherein the silicate has a d-spacing of from between about 10 to about 50 Angstroms as determined by X-Ray Diffraction (XRD).

14. The inorganic layered silicate of claim 13, wherein the layered silicate comprises at least one clay mineral.

15. The inorganic layered silicate of claim 14, wherein the clay mineral is a naturally-occurring clay.

16. The inorganic layered silicate of claim 14, wherein the clay mineral has an aspect ratio of between from about 50 to about 1000.

17. The inorganic layered silicate of claim 16, wherein the clay mineral has a thickness of about 1nm.

18. The inorganic layered silicate of claim 15, wherein the clay mineral is a smectite.

19. An inorganic layered silicate comprising a high temperature organic surfactant non-covalently attached to the silicate, the surfactant comprising a bromide salt of C_{18}-tributylphosphonium, wherein the silicate is a sodium salt of montmorillonite having an aspect ratio of about 50 to about 1000, a thickness of about 1 nm, and a d-spacing of from between about 10 to about 50 Angstroms as determined by X-Ray Diffraction (XRD).

20. The inorganic layered silicate of claim 19, wherein the ratio of the moles of the phosphonium salt to the moles of the montmorillonite salt is between from about 0.1 to at least about 10.

21. A nanocomposite comprising at least one of:

a) at least one of an inorganic layered silicate having at least one onium salt, or an organically modified layered aluminosilicate (ORMLAS); and

b) an intercalated or exfoliated polymer material,

wherein the nanocomposite has a heat distortion temperature of at least about 150°C.

22. The nanocomposite of claim 21, wherein the heat distortion temperature of the nanocomposite is between from about 250°C to about 400°C.

23. The nanocomposite of claim 21, wherein the polymer material is exfoliated within layers of the silicate and the silicate layers exhibit a d-spacing higher than about 18 to about 19 Angstroms or more as determined by X-Ray Diffraction (XRD).

24. The nanocomposite of claim 21, wherein the inorganic layered silicate is a naturally-occuring clay mineral.

25. The nanocomposite of claim 21, wherein said at least one onium salt has the following general formula:

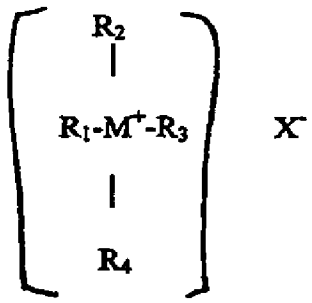

wherein M is N, O, S or P,

each of R1, R2, R3 and R4 is independently an optionally substituted or unsubstituted alkyl, alkenyl, alkynyl, cycloalkyl, cycloalkenyl, cycloalkynyl, aryl, alkylaryl, alkenylaryl, alkynylaryl, alkylthio, alkylsulfinyl, alkylsulfonyl, or carboxycyclic aryl group; in which each of R1, R2, R3 and R4 can be the same or different; and X^- is a counter ion.

26. The nanocomposite of claim 25, wherein the nanocomposite comprises said at least one onium salt and the moles of the onium salt are less than the moles of the silicate in the nanocomposite.

27. The nanocomposite of claim 21, wherein the nancomposite comprises at least one of said ORMLAS, the layered silicate of the ORMLAS having an aspect ratio of from between about 10 to about 1000.

28. The nanocomposite of claim 27, wherein the ORMLAS has a thickness of about 1nm to about 10nm.

29. The nanocomposite of claim 21, wherein the nancomposite comprises at least one of said ORMLAS, the layered silicate of the ORMLAS having a d-spacing of at least about 20 Angstroms.

30. The nanocomposite of claim 21, wherein nancomposite comprises at least one of said ORMLAS, the ORMLAS comprising at least one metal alkyl silsesquioxane.

31. The nanocomposite of claim 30, wherein the ORMLAS comprises at least one of alumino- octyl, dodecyl, or octadecyl silsesquioxane.

32. The nanocomposite of claim 21, wherein the polymer material is a polyamide, polyolefin, polyetherimide (PEI), thermoplastic polyimide, polysulfone, liquid crystal polymer, polyester, co-polyester, polyurethane, polyurethane copolyester copolymer, polypropylene (PP), polyethylene tetraphthalate (PET), polycarbonate (PC), Hytrel (butylene/poly (alkylene ether) phthalate plus stabilizer), Texin (polyurethane (PU)), Udel (polysulfone (PSU)), Vectra A or B (liquid crystal ploymer (LCP)), polyvinylchloride (PVC), polyvinylidene chloride (PVDC), polypthalamide (PPA), polyphenylene sulfide (PPS), Ultem (polyethermide), ethylenevinylalcohol (EVOH); or a blend or an alloy thereof.

33. The nanocomposite of claim 32, wherein the Hytrel polymer is selected from the group consisting of: Hytrel 5526, Hytrel 5612, Hytrel 4056, Hytrel 5526, and Hytrel 5612.

34. A nanocomposite having a heat distortion temperature of at least 150°C and comprising:

a) an inorganic layered silicate comprising a sodium salt of montmorillonite and a bromide salt of hexadecyltributyphosphonium; and

b) Ultem 1010 (polyetherimide) intercalated or exfoliated within layers of the silicate,

wherein the silicate layers exhibit a d-spacing higher than about 18 to about 19 Angstroms or more as determined by X-Ray Diffraction (XRD).

35. The nanocomposite of claim 34, wherein the ratio of the moles of the hexadecyltributyphosphonium salt to the moles of the silicate is between from about 0.1 to at least about 10.

36. A nanocomposite having a heat distortion temperature of at least 150°C and comprising:

a) an organically modified layered aluminosilicate (ORMLAS) comprising a C_{12}-alkyl silsesquioxane; and

b) Ultem 1010 (polyetherimide) intercalated or exfoliated within layers of the ORMLAS,

wherein ORMLAS comprises a layered silicate having a d-spacing of at least about 20 Angstroms as determined by X-ray Diffraction (XRD).

37. A nanocomposite comprising at least one of:

a) at least one inorganic layered silicate having at least one onium salt, or an organically modified layered aluminosilicate (ORMLAS); and

b) an intercalated or exfoliated polymer material,

wherein the high gas or a liquid transmission rate through the nanocomposite is at least about 1.5 fold lower than the polymer material (neat).

38. The nanocomposite of claim 37, wherein the gas transmission rate through the nanocomposite is at least about 10 to about 200 fold less than the polymer material (neat) as determined by a standard gas transmission rate test.

39. The nanocomposite of claim 38, wherein the gas is oxygen, nitrogen, carbon dioxide, water vapor, a noble gas, or a mixture thereof.

40. The nanocomposite of claim 39, wherein the noble gas is helium.

41. The nanocomposite of claim 40, wherein the helium transmission rate through the nanocomposite is less than about 20×10^{-8} $cm.cm^3/sec.cm^2.atm$

42. The nanocomposite of claim 39, wherein the transmission rate of the water vapor through the nanocomposite is up to about 20 times lower than the polymer material (neat) as determined by a standard water vapor transmission rate test.

43. The nanocomposite of claim 39, wherein the transmission rate of the oxygen through the nanocomposite is up to about 100 fold less than the polymer material (neat) as determined by a standard oxygen gas transmission rate test.

44. The nanocomposite of claim 37, wherein the nanocomposite comprises between from about 0.1% (w/w) to about 10% (w/w) of at least one clay mineral.

45. The nanocomposite of claim 44, wherein the clay mineral is a naturally-occuring clay in an amount of about 5% (w/w).

46. The nanocomposite of claim 45, wherein the layered silicate has an interlayer d-spacing of between from about 1 to about 5nm as determined by X-Ray Diffraction (XRD).

47. The nanocomposite of claim 37, wherein polymer material is a polyamide, polyolefin, polyetherimide (PEI), thermoplastic polyimide, polysulfone, liquid crystal polymer, polyester, co-polyester, polyurethane, polyurethane copolyester copolymer, polypropylene (PP), polyethylene tetraphthalate (PET), polycarbonate (PC), Hytrel (butylene/poly (alkylene ether) phthalate plus stabilizer), Texin (polyurethante (PU), Udel (polysulfone (PSU), Vectra A or B (liquid crystal ploymer (LCP), polyvinylchloride (PVC), polyvinylidene cloride (PVDC), polypthalamide (PPA), polyphenylene sulfide (PPS), Ultem (polyethermide), ethylenevinylalcohol (EVOH); or a blend or an alloy thereof.

48. The nanocomposite of claim 47, wherein the Hytrel polymer is selected from the group consisting of: Hytrel 5526, Hytrel 5612, Hytrel 4056, Hytrel 5526, and Hytrel 5612.

49. A nanocomposite comprising:

a) a sodium salt of montmorillonite comprising dimethyl-hydrogenated tallow (2-ethyl hexyl) ammonium and methyl tallow bis-2 hydroxyethyl ammonium; and

b) an intercalated or exfoliated polymer material consisting of polyethylene tetraphthalate (PET), polyolefin, or ethylenevinylalcohol (EVOH), the amount of the polymer material being about 5% (w/w) of the nanocomposite,

wherein,

c) the oxygen permeability of the nanocomposite is about 100 fold less than the permeability of polymer material to oxygen as determined by a standard gas permeability test, or

d) the water vapor permeability of the nanocomposite is about 20 fold less than permeability of polymer material to water vaper as determined by the test.

50. The nanocomposite of claim 21 or 37, wherein the nanocomposite exhibits an impact resistance of at least about 10% higher than polymer material (neat).

51. The nanocomposite of claim 21 or 37, wherein the nanocomposite exhibits a tensile modulus of at least about 10% higher than polymer material (neat).

52. The nanocomposite of claim 21 or 37, wherein the nanocomposite exhibits a flame resistance of at least about 10% higher than the polymer material (neat).

53. The nanocomposite of claim 21 or 37, wherein the nanocomposite exhibits a glass transition temperature (T_g) of at least about 10% higher than polymer material (neat).

54. The nanocomposite of claim 21 or 37, wherein the nanocomposite exhibits a melting temperature (T_m) of at least about 10% higher than the polymer material (neat).

55. An article of manufacture comprising at least one of the nanocomposites of claim 21 or 37.

56. The article of manufacture as recited in claim 55, wherein the article is adapted for pharmaceutical, medical, research, automotive, aircraft, spacecraft apparel, eyewear, furniture, construction, packaging or marine use.

57. The article of manufacture as recited in claim 56, wherein the article is adapted to enclose at least one of a gas, liquid, semi-solid, or solid material.

58. The article of manufacture as recited in claim 57, wherein the article is a bottle or pouch implementation adapted to enclose the material.

59. The article of manufacture as recited in claim 58, wherein the liquid is a dairy product, fruit juice, soft drink, or a pharmaceutical.

60. The article of manufacture of claim 57, wherein the pouch implementation is a blister pack.

61. The article of manufacture of claim 60, wherein the blister pack exhibits a gas permeability that is at least 1.5 fold less than the neat polymer as determined by a standard solute transmission rate test.

62. A polyolefin-layered silicate polymer nanocomposite (polymer alloy nanocomposite) comprising: 1) between from about 40 to about 99% polyolefin by weight of nanocomposite; 2) between from about 1 to about 55% polyamide by weight of the polyolefin; 3) between from about 0.5 to about 25% functionalized grafted polyolefin by weight of polyamide polymer; 4) between from about 1 to

about 40% organoclay by weight of the polyolefin; and 5) between from about 0 to about 25% synthetically formulated organoclay by weight of the polyolefin.

63. A method of making the polymer alloy nanocomposite of claim 62 comprising compounding polymer blend components in an extruder at a temperature of at least 190°C and extruding the polymer alloy nanocomposite.

CURRENT
STATE-OF-THE-ART
TEMP. LIMIT = 100-150°C

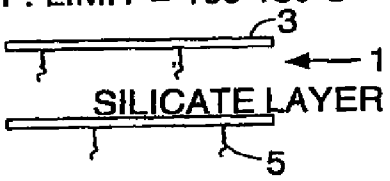

ALKYL AMMONIUM
SURFACTANTS

FIG. 1A

APPROACH
TEMP. LIMIT = 200°C

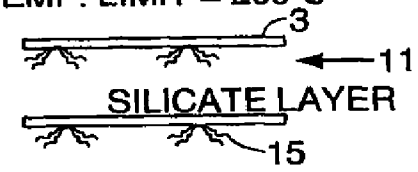

TETRAPHENYL PHOSPHONIUM
SURFACTANTS

FIG. 1B

APPROACH
TEMP. LIMIT > 250°C

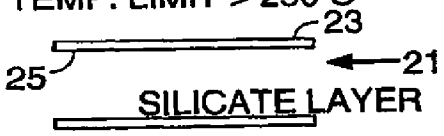

SURFACTANT-FREE ORGANOPHILIC
LAYERED SILICATE

FIG. 1C

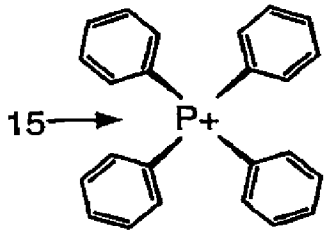

CHEMICAL STRUCTURE OF TRITON SYSTEMS'
TETRAPHENYL PHOSPHONIUM SURFACTANT

FIG. 2

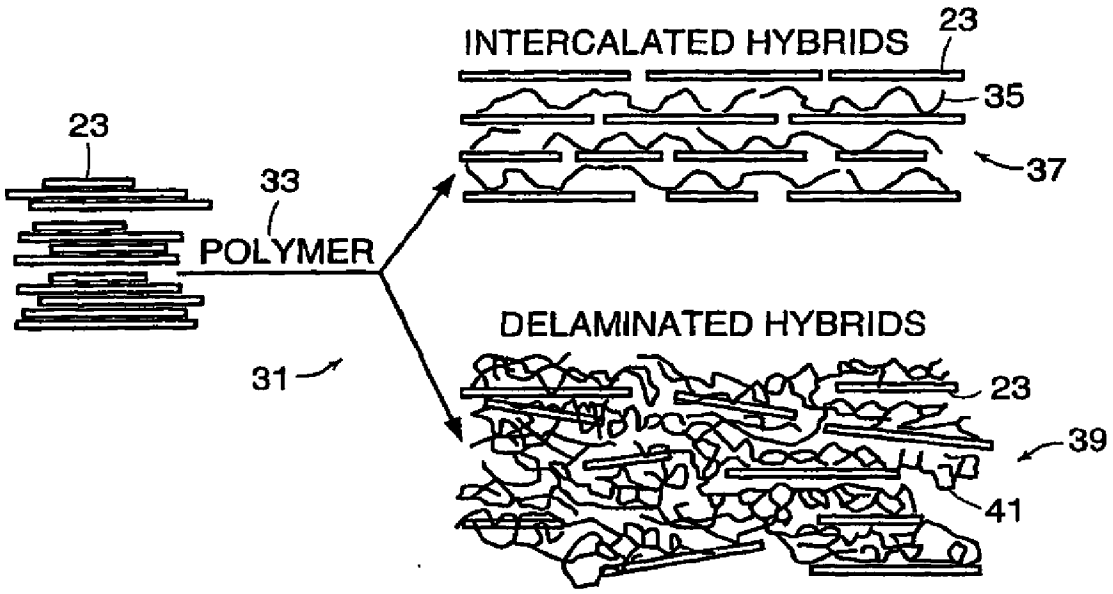

SCHEMATIC OF POLYMER-LAYERED SILICATE NANOCOMPOSITE STRUCTURES

FIG. 3

PROPERTIES OF NYLON-6 AND LAYERED SILICATE-NYLON NANOCOMPOSITES

PROPERTY	NANOCOMPOSITE	*NEAT* NYLON-6
TENSILE MODULUS (GPa)	2.1	1.1
TENSILE STRENGTH (MPa)	107	69
HEAT DISTORTION TEMPERATURE (°C)	145	65
IMPACT STRENGTH (kl/m^2)	2.8	2.3
WATER ABSORPTION (%)	0.51	0.87
COEFFICIENT OF THERMAL EXPANSION (x,y)	6.3 X 10-5	13 X 10-5

FIG. 4

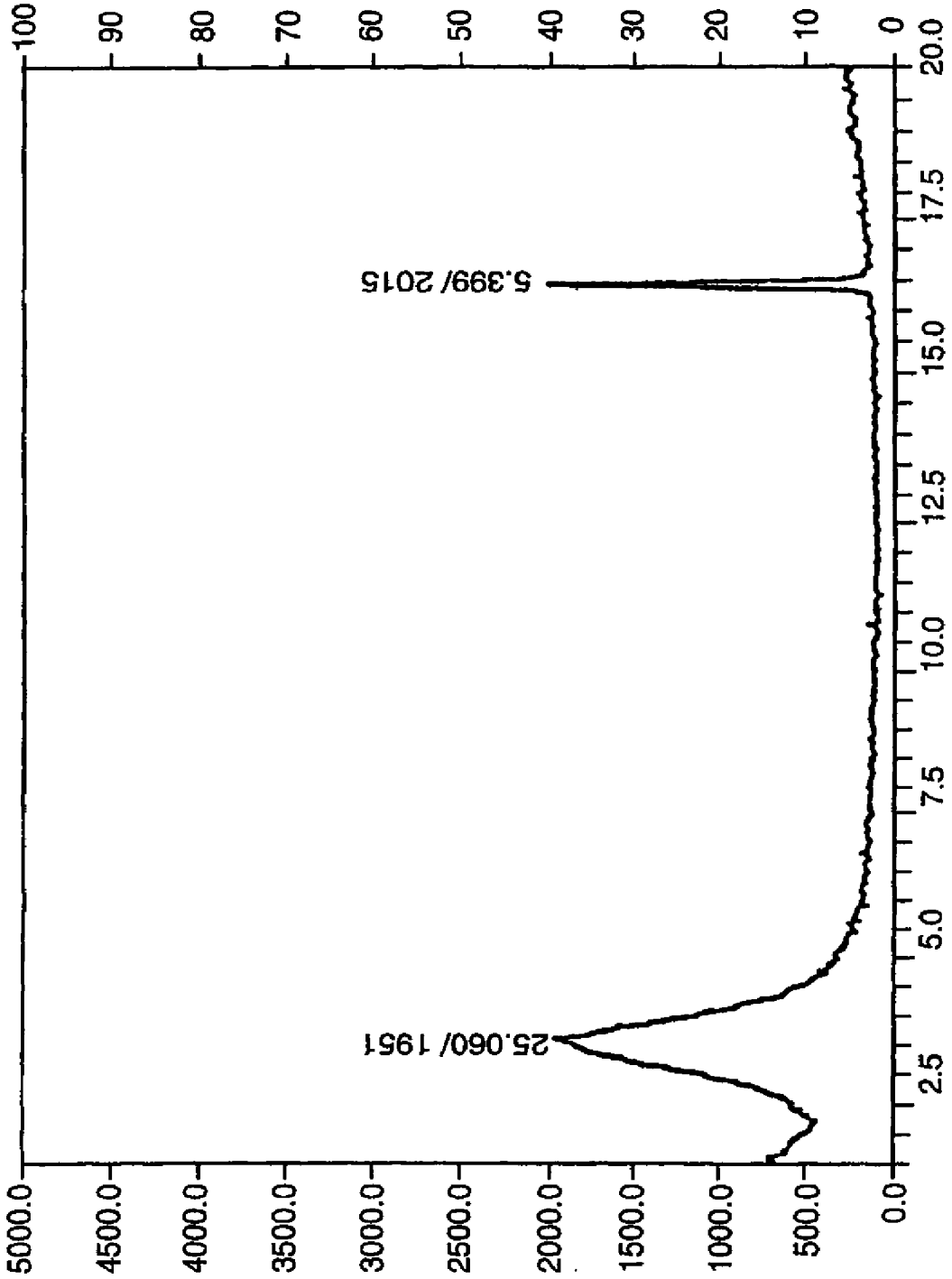
5.399/ 2015
25.060/ 1951
100
90
80
70
60
50
40
30
20
10
0
20.0
17.5
15.0
12.5
10.0
7.5
5.0
2.5
5000.0
4500.0
4000.0
3500.0
3000.0
2500.0
2000.0
1500.0
1000.0
500.0
0.0

FIG. 5

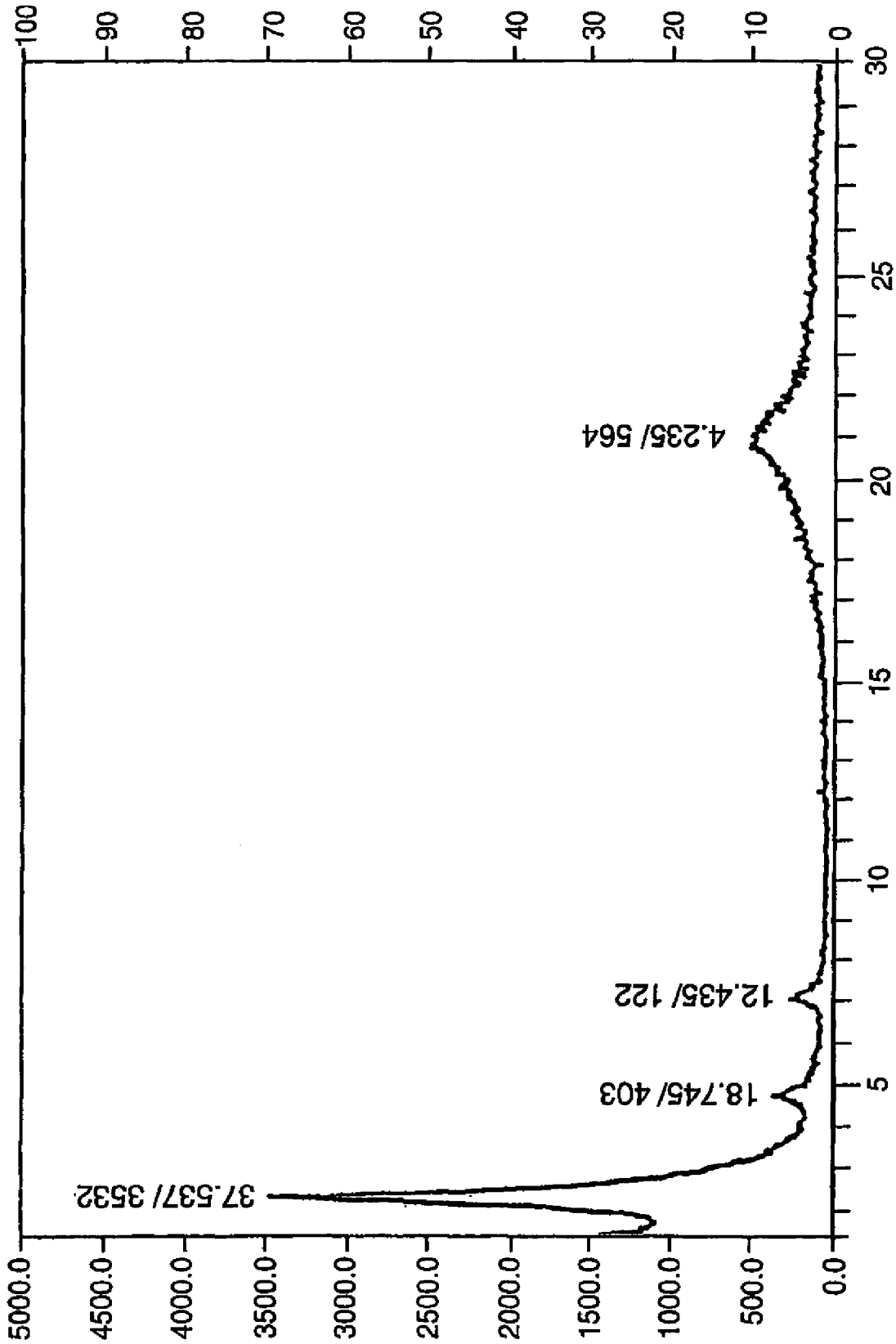
37.537/ 3532
18.745/ 403
12.435/ 122
4.235/ 564
5000.0
4500.0
4000.0
3500.0
3000.0
2500.0
2000.0
1500.0
1000.0
500.0
0.0
100
90
80
70
60
50
40
30
20
10
0
30
25
20
15
10
5

FIG. 6

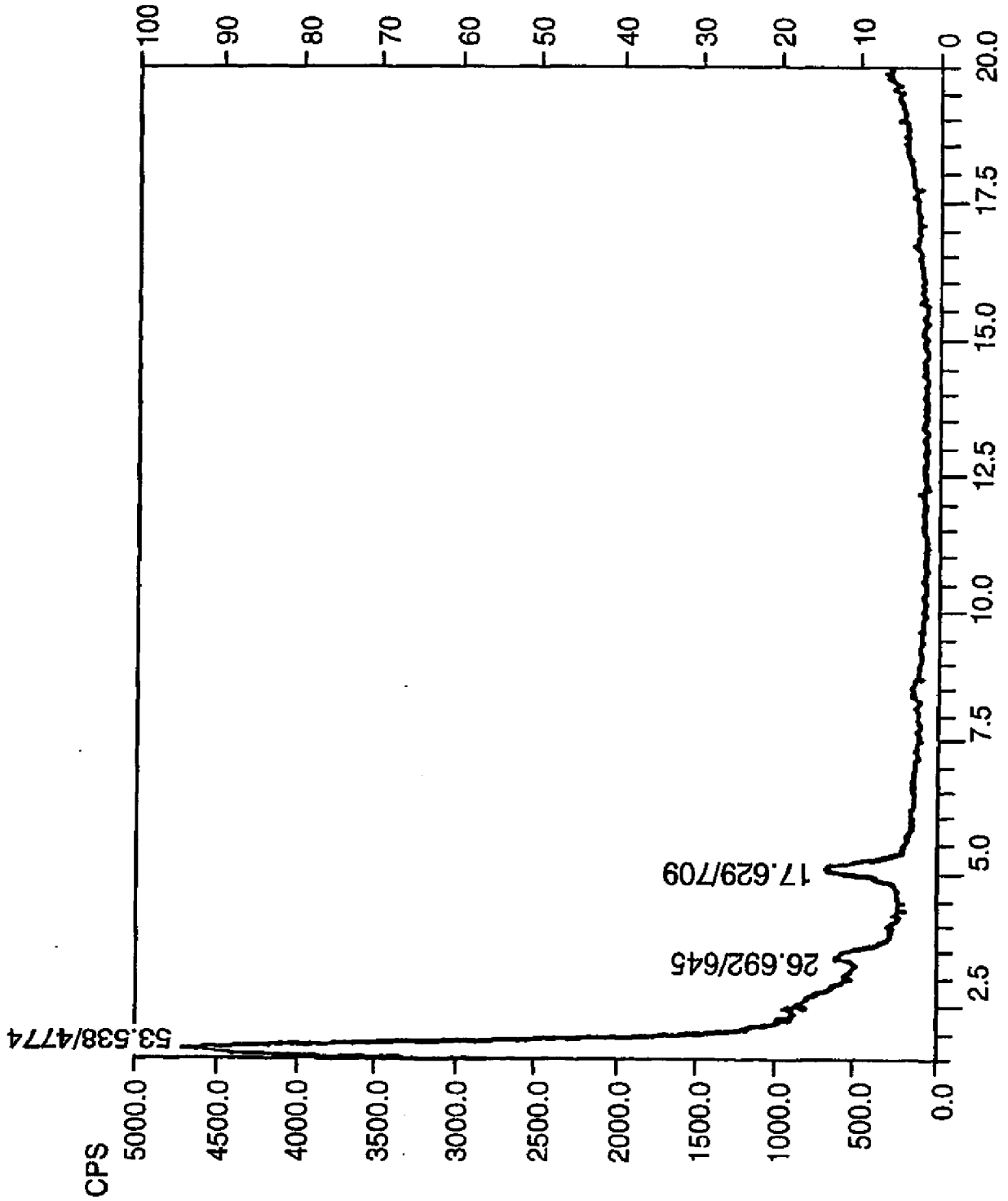
CPS
5000.0
4500.0
4000.0
3500.0
3000.0
2500.0
2000.0
1500.0
1000.0
500.0
0.0
2.5
5.0
7.5
10.0
12.5
15.0
17.5
20.0
0
10
20
30
40
50
60
70
80
90
100
53.538/4774
26.692/645
17.629/709

FIG. 7

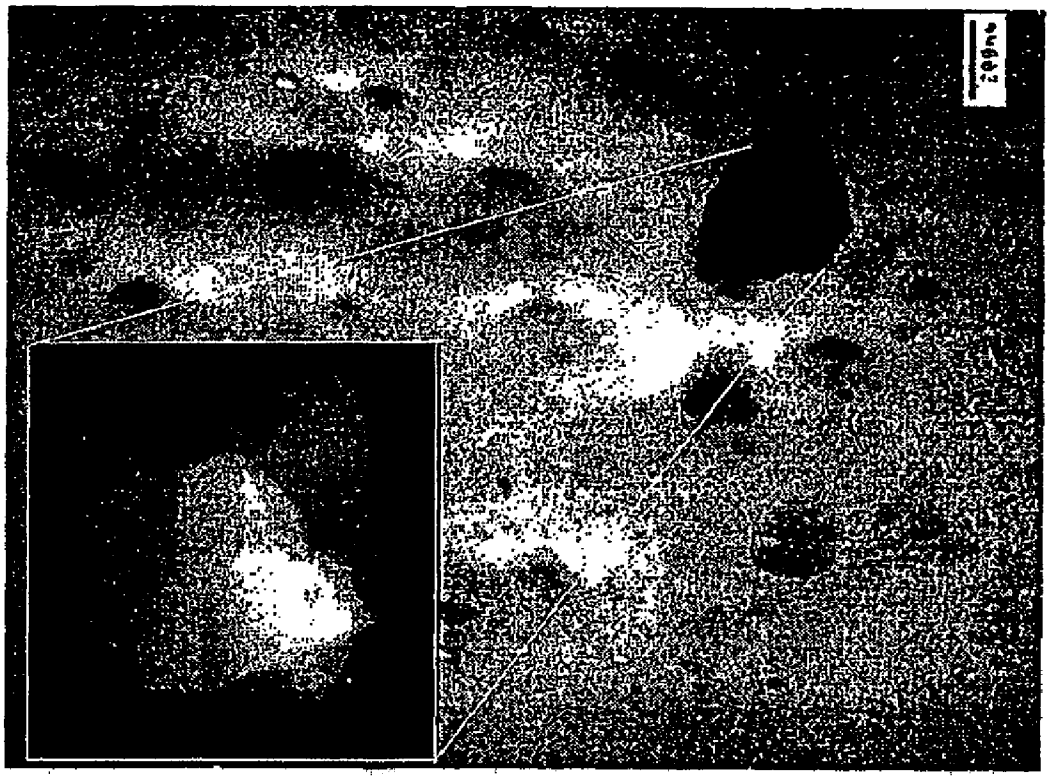

FIG. 9

FIG. 8

FIG. 11

FIG. 10

	Silane 1	Silane 2	d spacing
a	Octyl		25.1 Å
b	Dodecyl 1		37.5 Å
c	Dodecyl 2		38.6, 29.8 Å
d	Hexadecyl		47.2 Å
e	Octadecyl		53.5 Å
f	Phenethyl		22.9 Å (broad)
g	Phenyl		20.0 Å (broad)
h	Phenethyl (75%)	Dodecyl	25.9 Å
i	Phenethyl (50%)	Dodecyl	27.4 Å
j	Phenethyl (25%)	Dodecyl	35.9 / 29.4 Å

FIG. 12

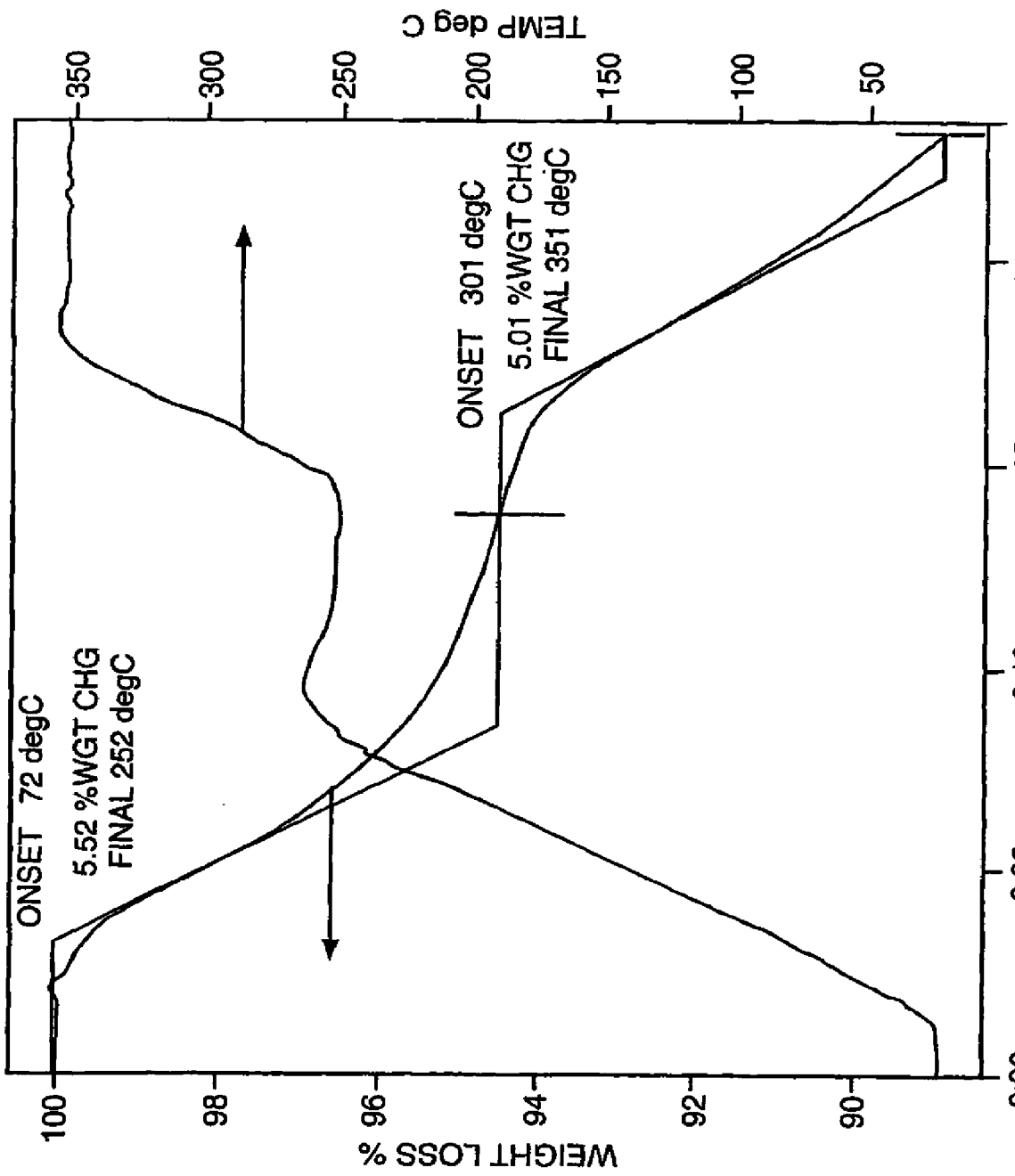
TEMP deg C
350
300
250
200
150
100
50
ONSET 72 degC
5.52 %WGT CHG
FINAL 252 degC
ONSET 301 degC
5.01 %WGT CHG
FINAL 351 degC
WEIGHT LOSS %
100
98
96
94
92
90
0:00
0:08
0:10
0:25
0:33
TIME (HRS:MIN)

FIG. 13

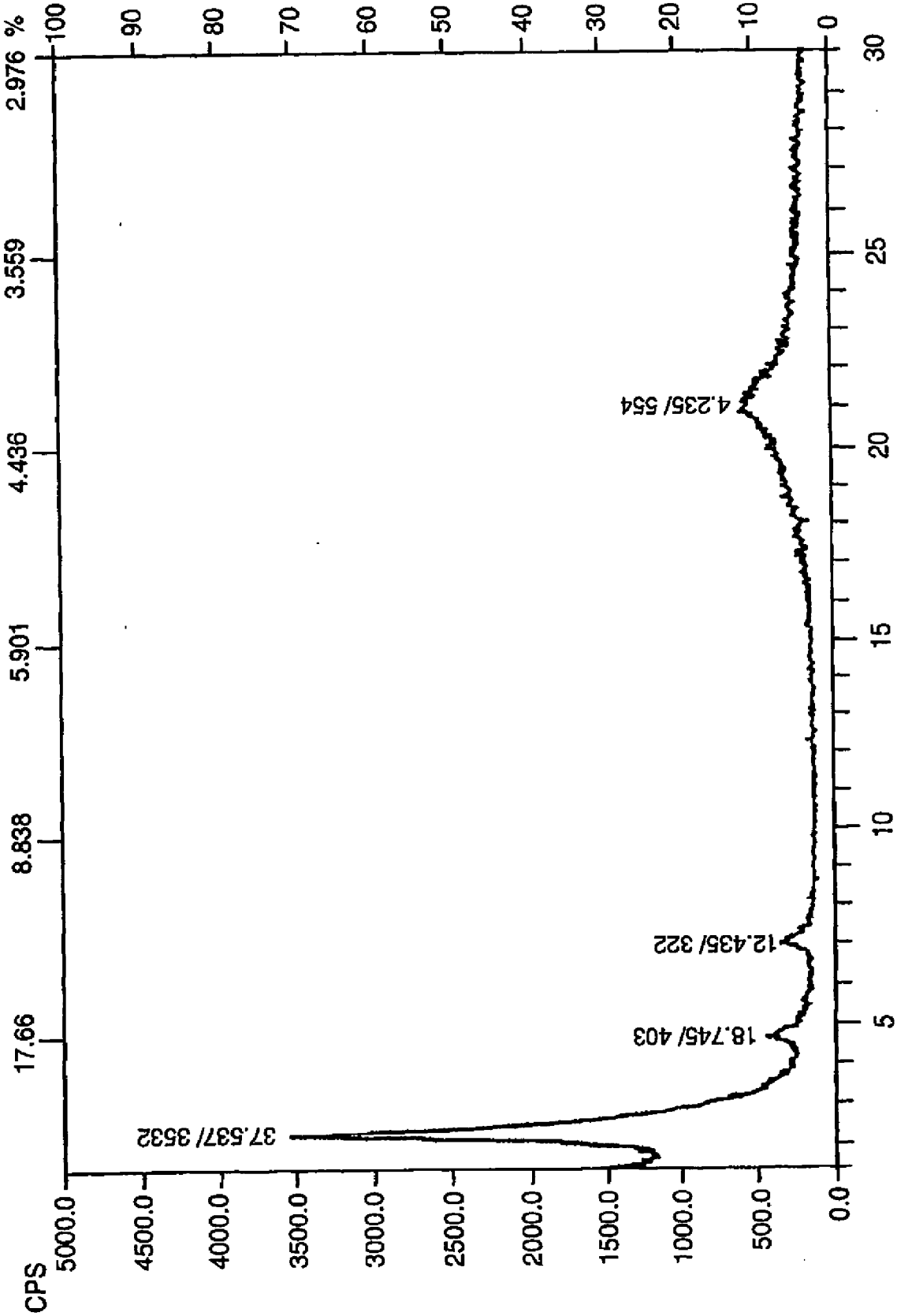
CPS
5000.0
4500.0
4000.0
3500.0
3000.0
2500.0
2000.0
1500.0
1000.0
500.0
0.0
%
100
90
80
70
60
50
40
30
20
10
0
2.976
3.559
4.436
5.901
8.838
17.66
37.537/ 3532
18.745/ 403
12.435/ 322
4.235/ 554
30
25
20
15
10
5

FIG. 14A

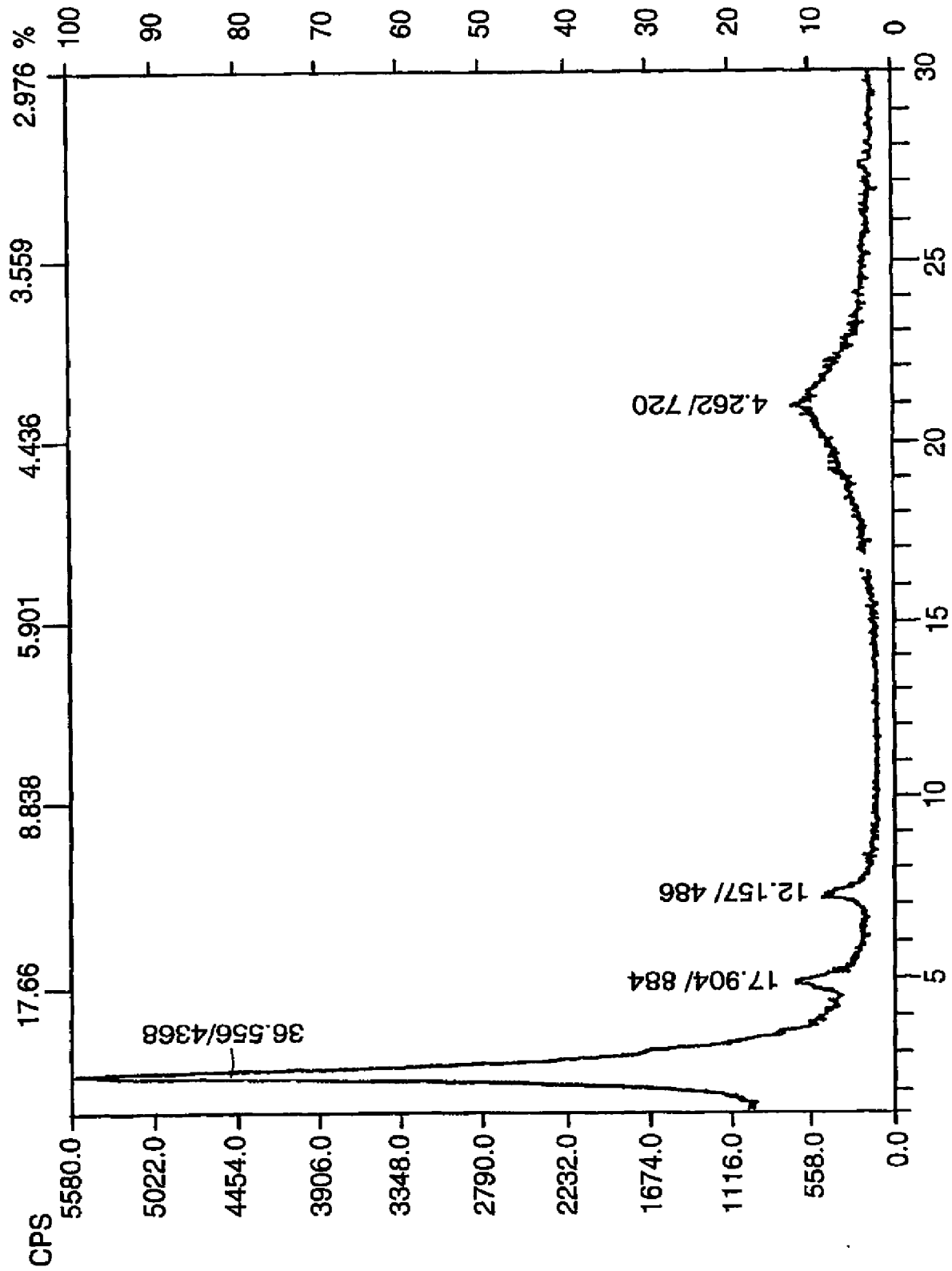
CPS
5580.0
5022.0
4454.0
3906.0
3348.0
2790.0
2232.0
1674.0
1116.0
558.0
0.0
%
100
90
80
70
60
50
40
30
20
10
0
2.976
3.559
4.436
5.901
8.838
17.66
30
25
20
15
10
5
36.556/4368
17.904/ 884
12.157/ 486
4.262/ 720

FIG. 14B

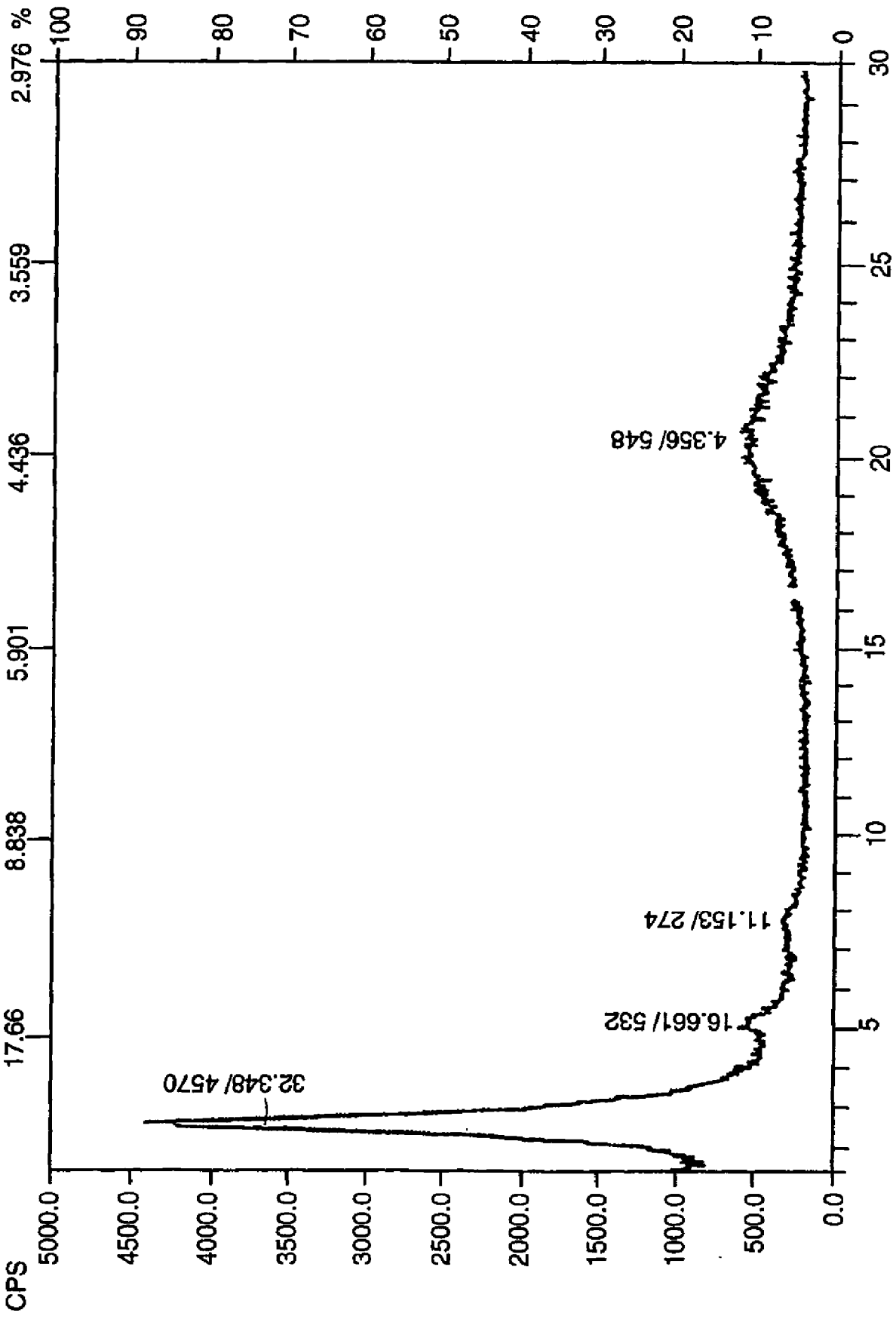
CPS
5000.0
4500.0
4000.0
3500.0
3000.0
2500.0
2000.0
1500.0
1000.0
500.0
0.0
2.976 %
100
90
80
70
60
50
40
30
20
10
0
3.559
4.436
5.901
8.838
17.66
30
25
20
15
10
5
0
32.348/ 4570
16.661/ 532
11.153/ 274
4.356/ 548

FIG. 14C

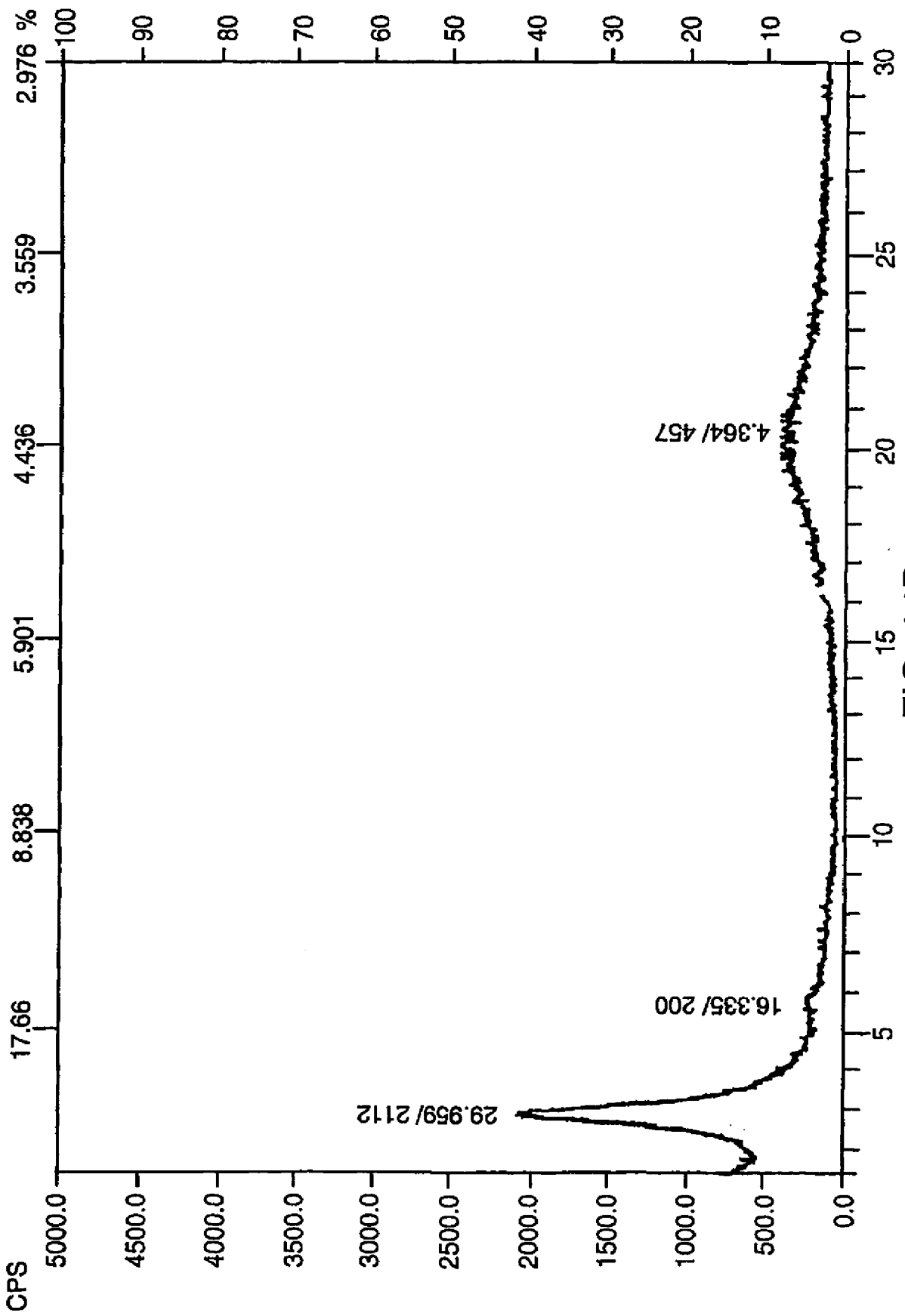
CPS
5000.0
4500.0
4000.0
3500.0
3000.0
2500.0
2000.0
1500.0
1000.0
500.0
0.0
2.976 %
3.559
4.436
5.901
8.838
17.66
100
90
80
70
60
50
40
30
20
10
0
30
25
20
15
10
5
29.959/ 2112
16.335/ 200
4.364/ 457

FIG. 14D

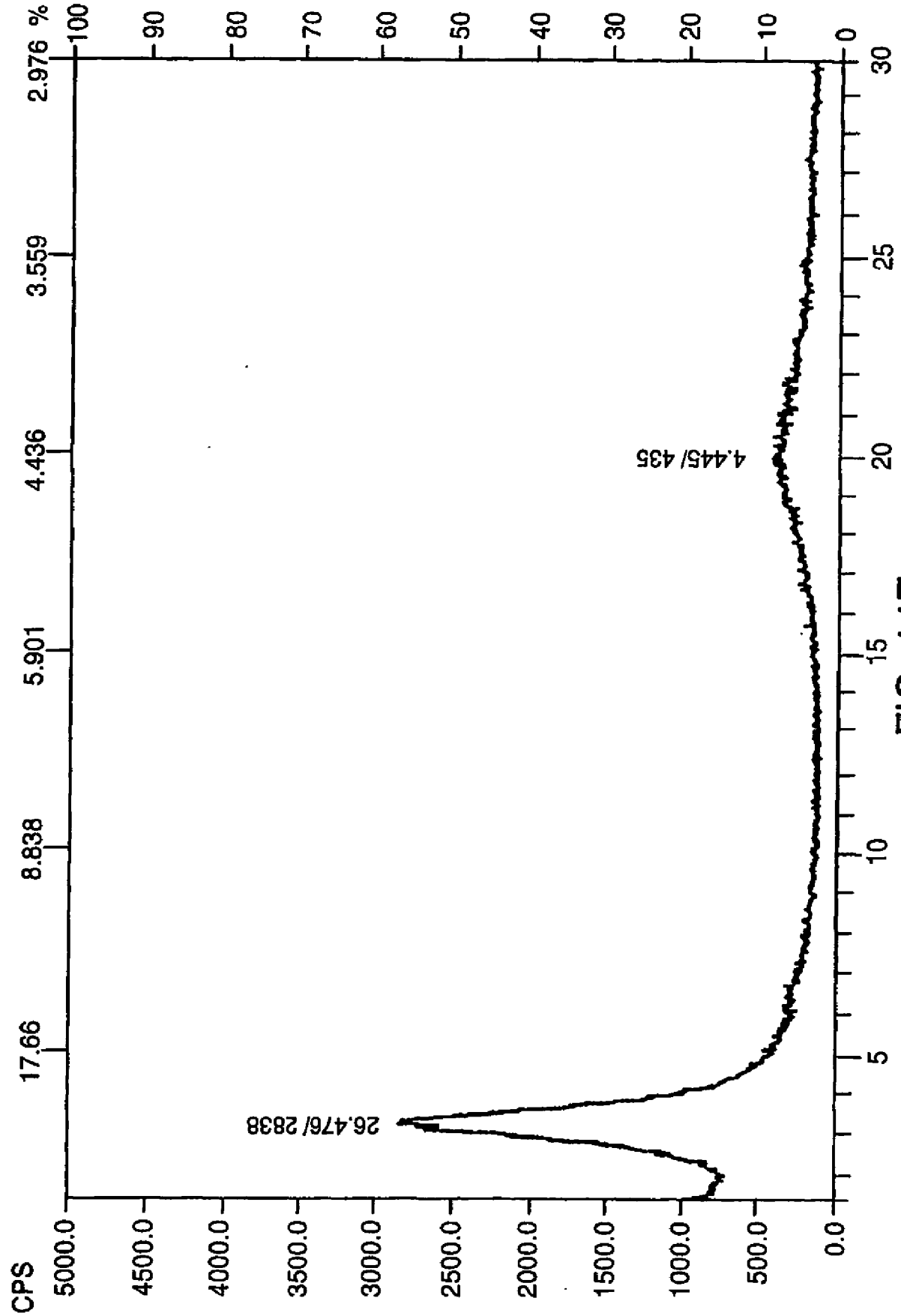
CPS
5000.0
4500.0
4000.0
3500.0
3000.0
2500.0
2000.0
1500.0
1000.0
500.0
0.0
17.66
8.838
5.901
4.436
3.559
2.976 %
100
90
80
70
60
50
40
30
20
10
0
30
25
20
15
10
5
26.476/ 2838
4.445/ 435

FIG. 14E

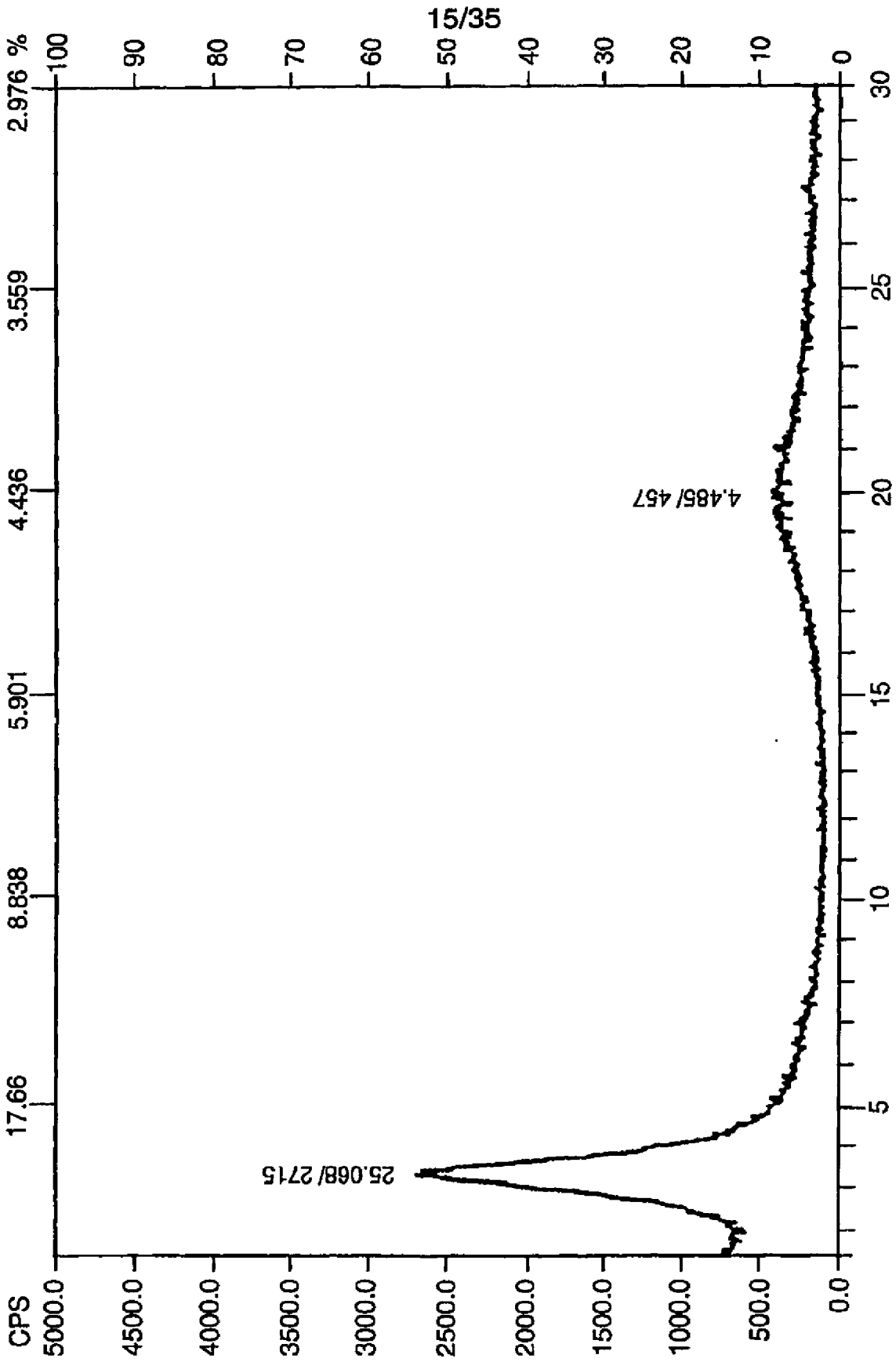
CPS
5000.0
4500.0
4000.0
3500.0
3000.0
2500.0
2000.0
1500.0
1000.0
500.0
0.0
17.66
8.838
5.901
4.436
3.559
2.976 %
100
90
80
70
60
50
40
30
20
10
0
5
10
15
20
25
30
25.068/ 2715
4.485/ 457

FIG. 14F

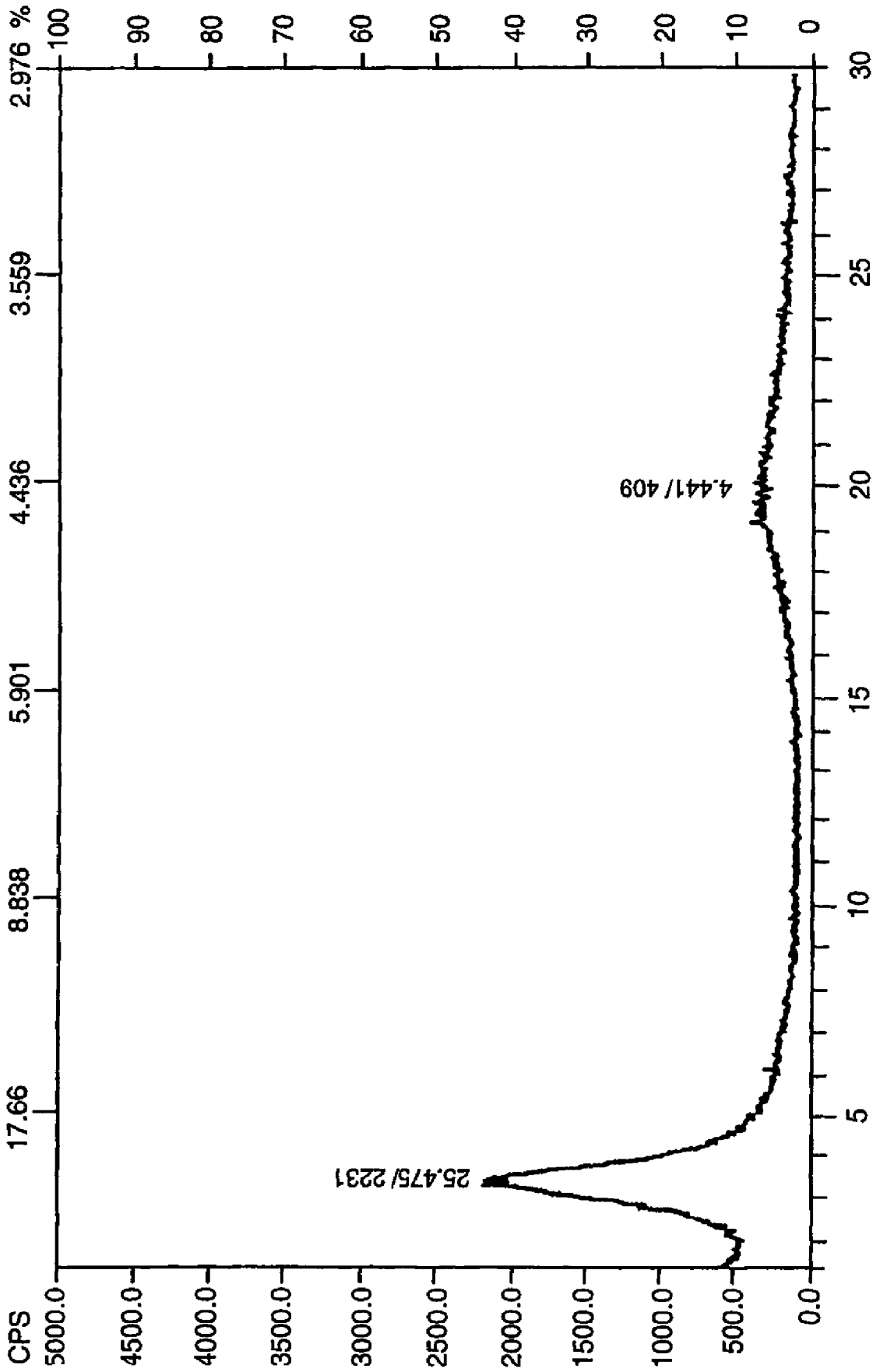
CPS
5000.0
4500.0
4000.0
3500.0
3000.0
2500.0
2000.0
1500.0
1000.0
500.0
0.0
17.66
8.838
5.901
4.436
3.559
2.976 %
100
90
80
70
60
50
40
30
20
10
0
5
10
15
20
25
30
25.475/ 2231
4.441/ 409

FIG. 14G

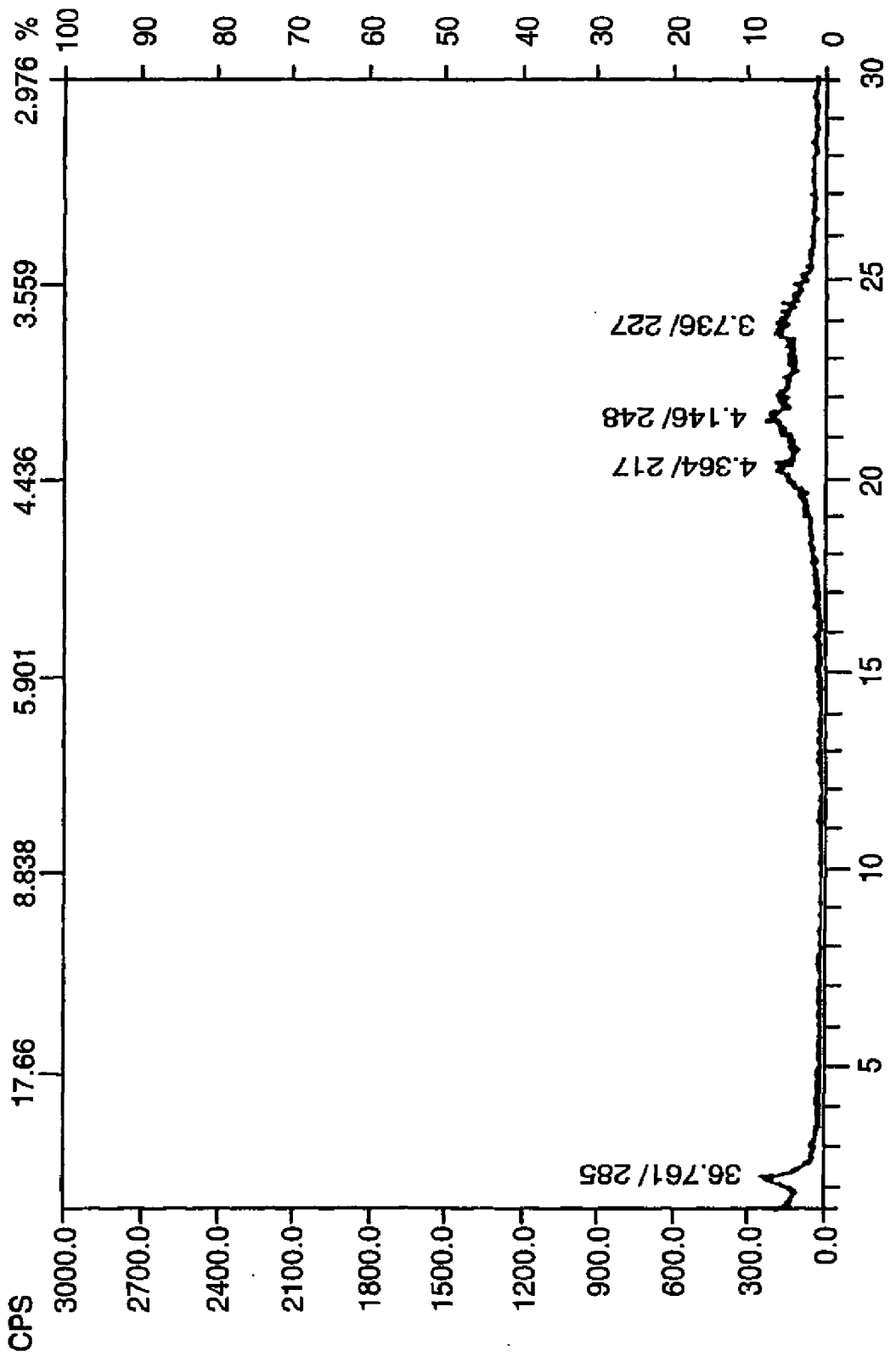
CPS
3000.0
2700.0
2400.0
2100.0
1800.0
1500.0
1200.0
900.0
600.0
300.0
0.0
17.66
8.838
5.901
4.436
3.559
2.976
%
100
90
80
70
60
50
40
30
20
10
0
5
10
15
20
25
30
36.761/ 285
4.364/ 217
4.146/ 248
3.736/ 227

FIG. 15A

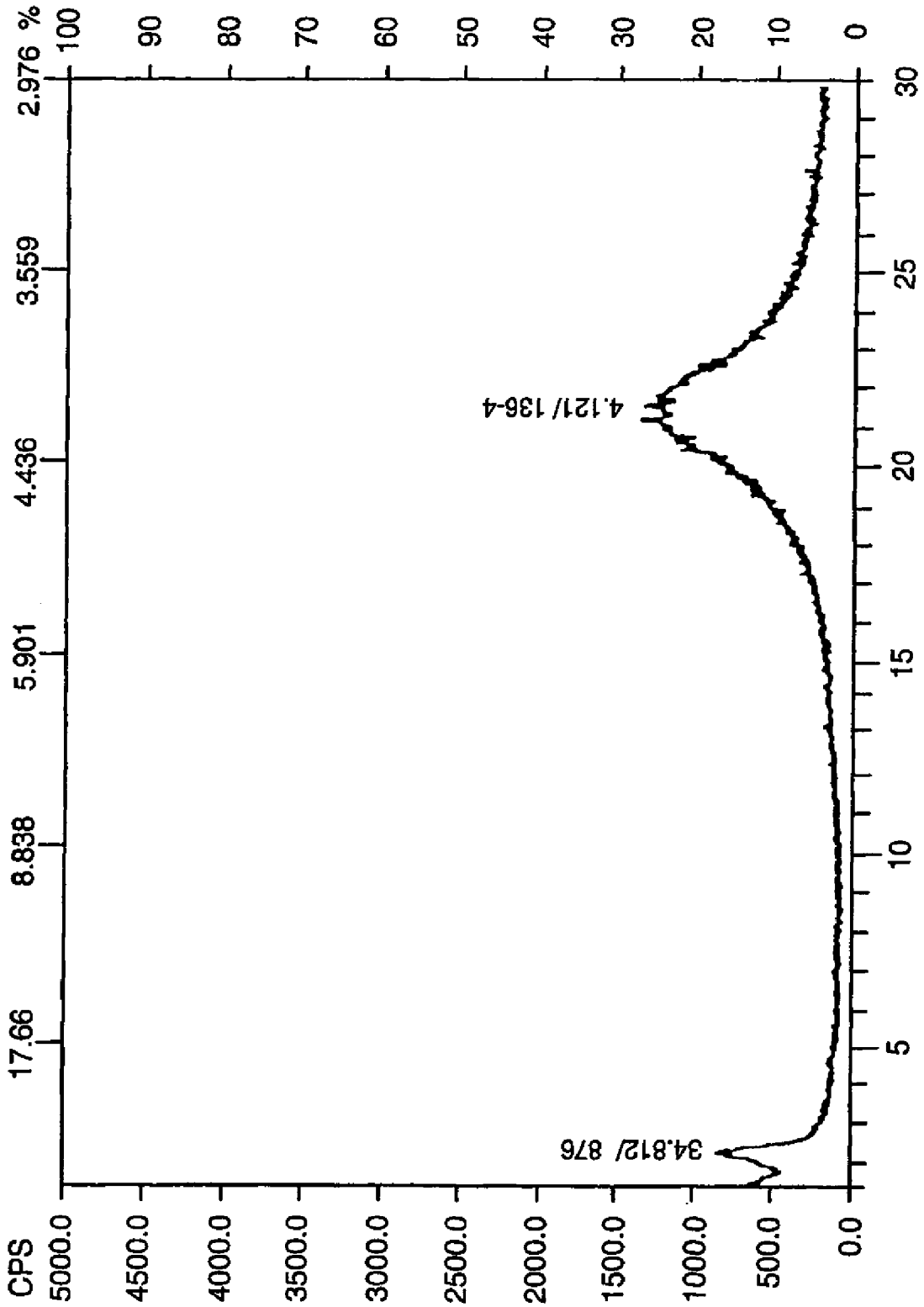
CPS
5000.0
4500.0
4000.0
3500.0
3000.0
2500.0
2000.0
1500.0
1000.0
500.0
0.0
17.66
8.838
5.901
4.436
3.559
2.976 %
100
90
80
70
60
50
40
30
20
10
0
5
10
15
20
25
30
34.812/ 876
4.121/ 136-4

FIG. 15B

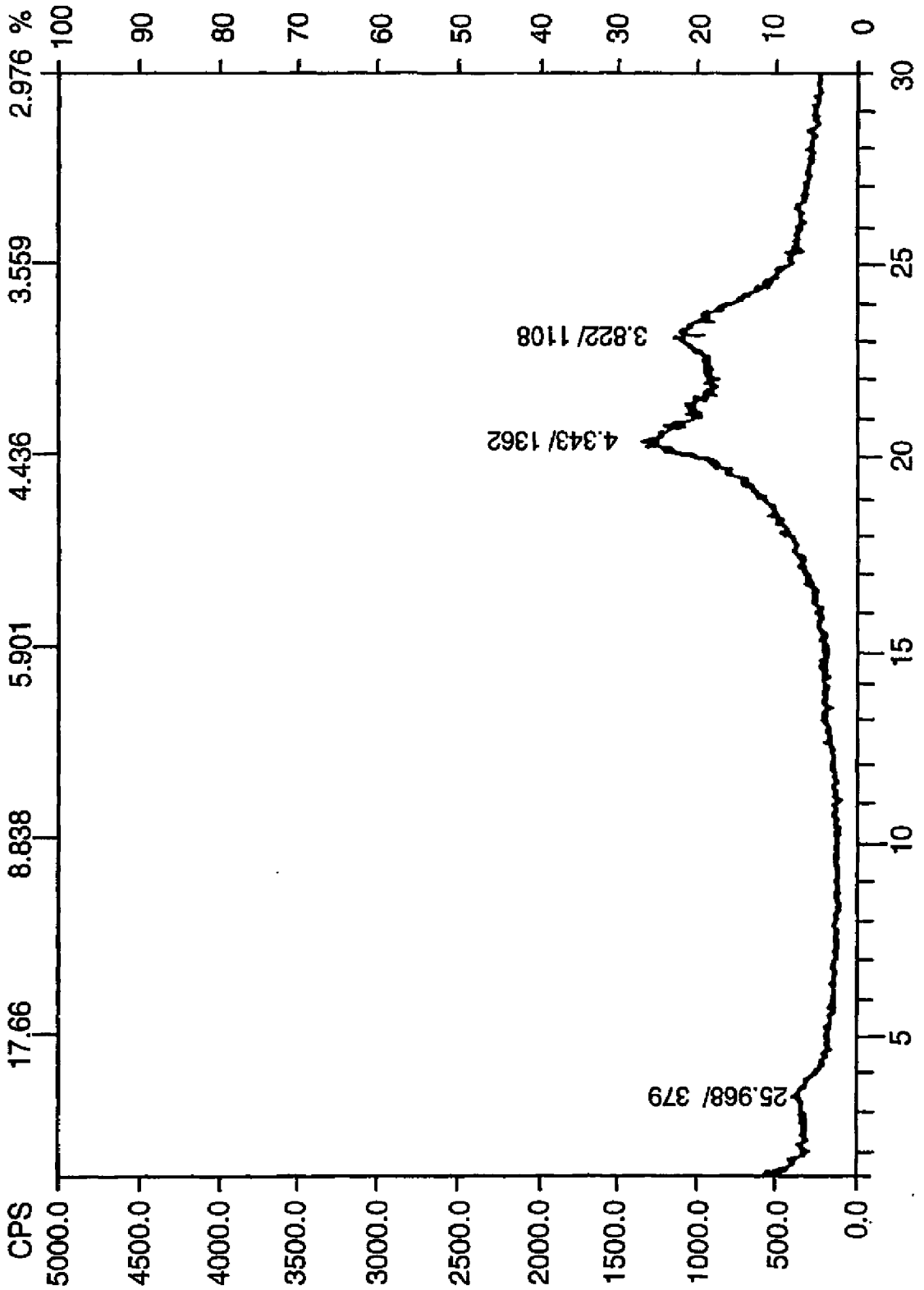
CPS
5000.0
4500.0
4000.0
3500.0
3000.0
2500.0
2000.0
1500.0
1000.0
500.0
0.0
17.66
8.838
5.901
4.436
3.559
2.976 %
100
90
80
70
60
50
40
30
20
10
0
5
10
15
20
25
30
25.968/ 379
4.343/ 1362
3.822/ 1108

FIG. 15C

FIG. 16B

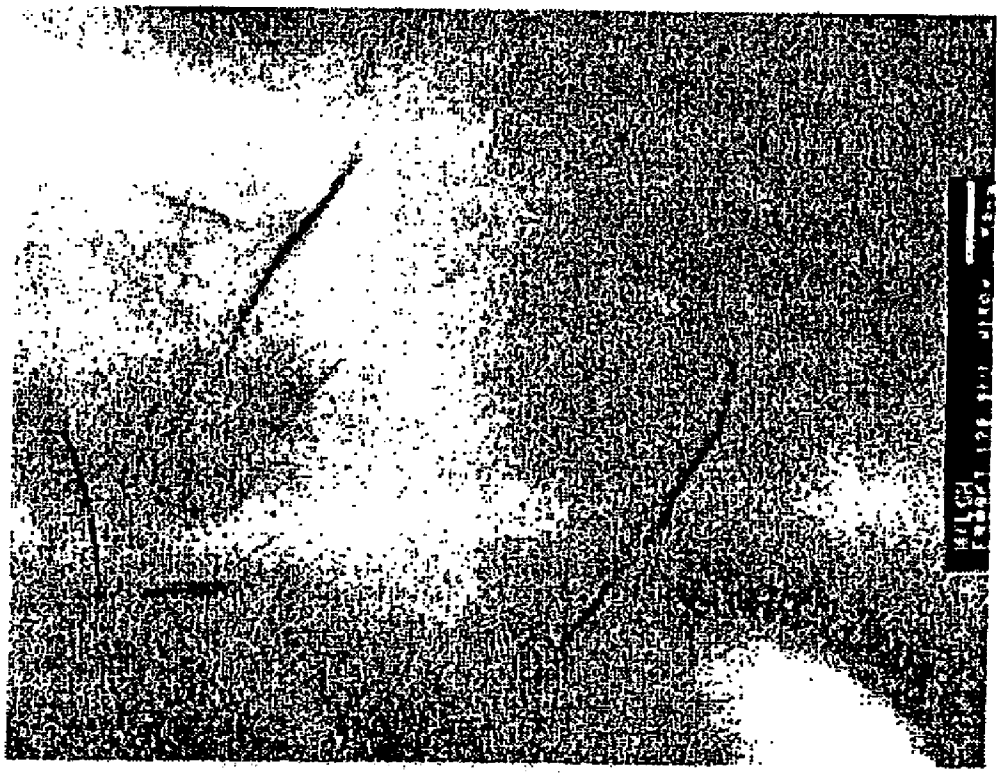

FIG. 16A

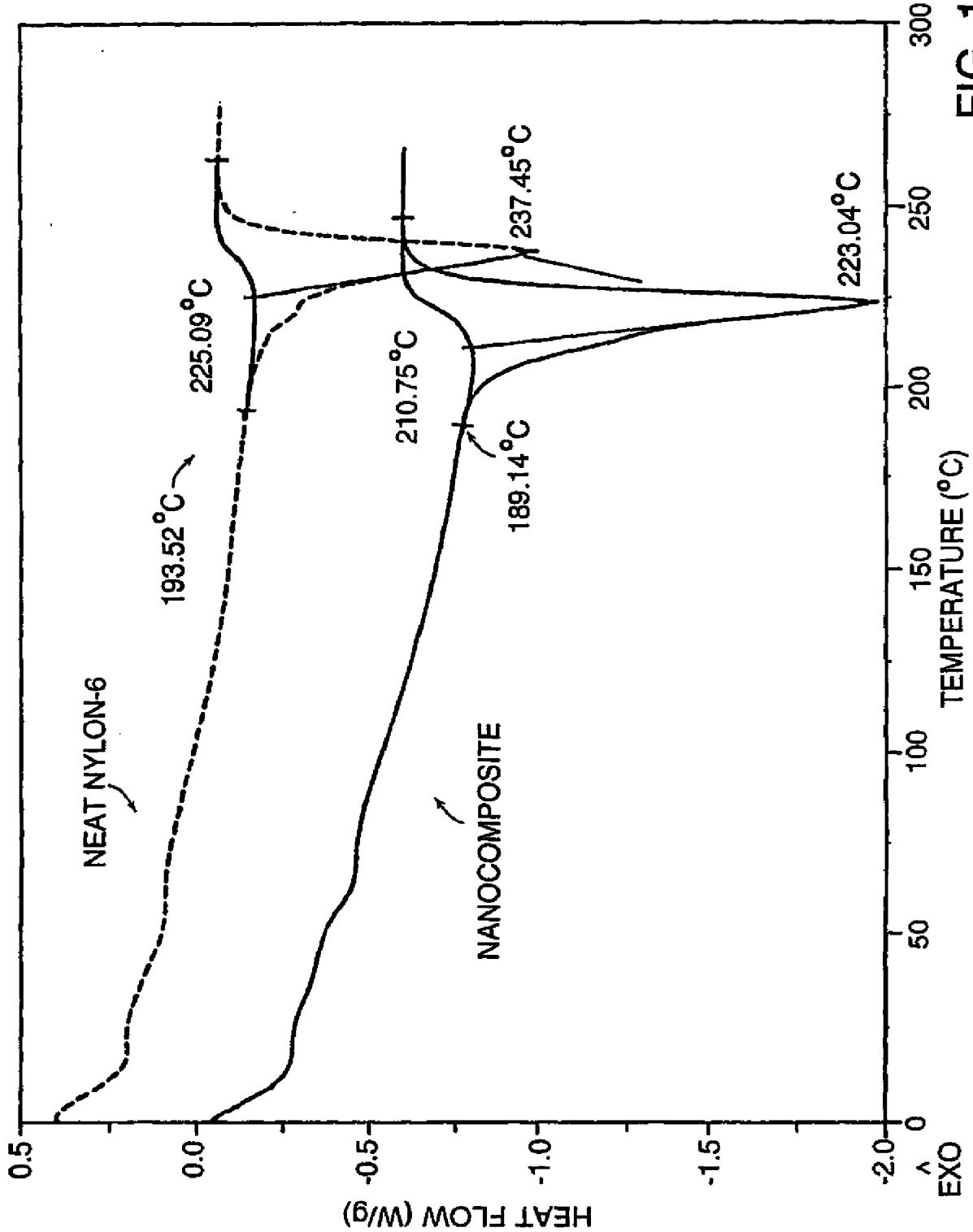
HEAT FLOW (W/g)
0.5
0.0
-0.5
-1.0
-1.5
-2.0
EXO
0
50
100
150
200
250
300
TEMPERATURE (°C)
NEAT NYLON-6
193.52°C
225.09°C
NANOCOMPOSITE
210.75°C
189.14°C
237.45°C
223.04°C

FIG. 17A

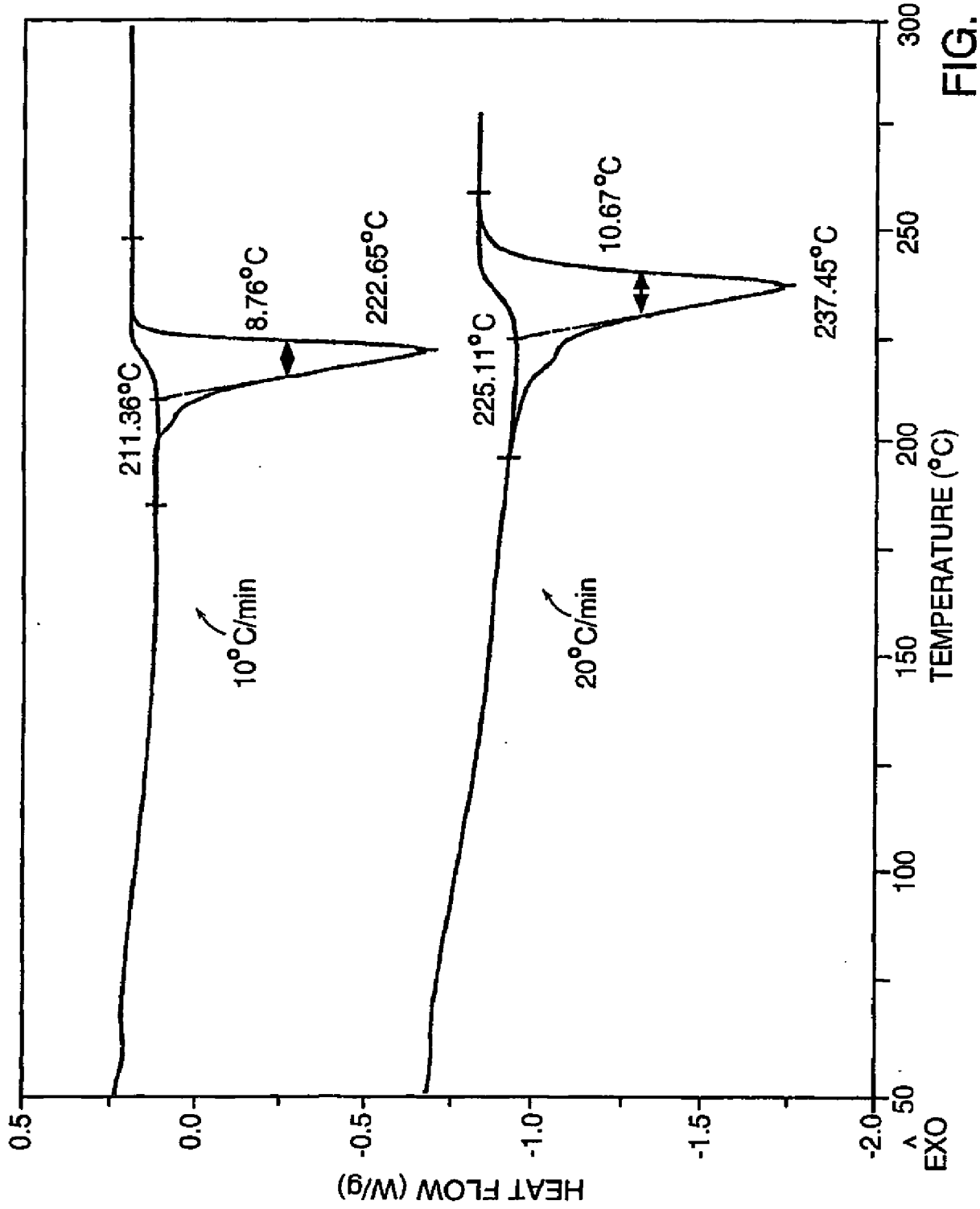
211.36°C
8.76°C
222.65°C
10°C/min
225.11°C
10.67°C
237.45°C
20°C/min
0.5
0.0
-0.5
-1.0
-1.5
-2.0
HEAT FLOW (W/g)
50
100
150
200
250
300
TEMPERATURE (°C)
EXO

FIG. 17B

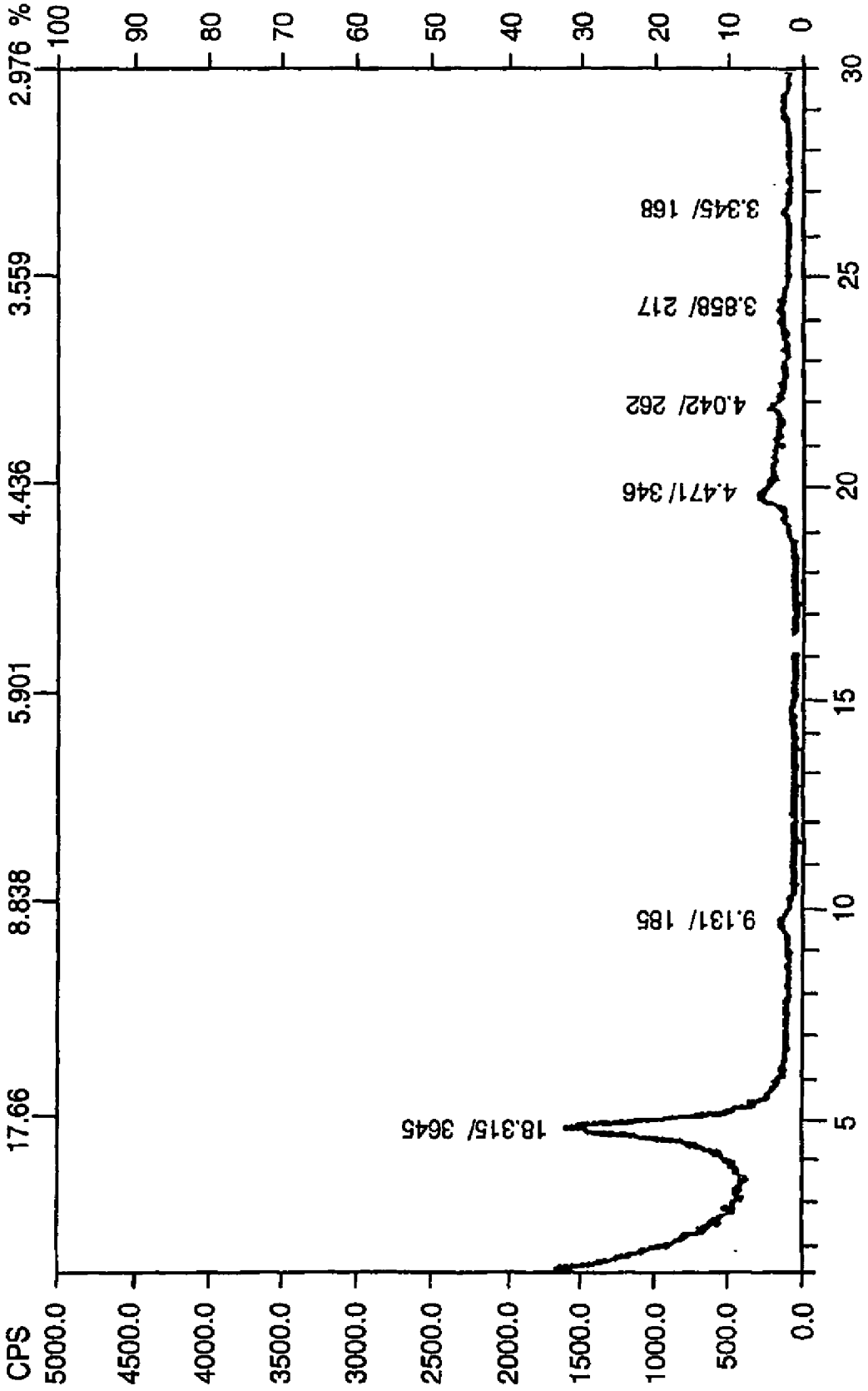
CPS
5000.0
4500.0
4000.0
3500.0
3000.0
2500.0
2000.0
1500.0
1000.0
500.0
0.0
17.66
8.838
5.901
4.436
3.559
2.976 %
100
90
80
70
60
50
40
30
20
10
0
5
10
15
20
25
30
18.315/ 3645
9.131/ 185
4.471/ 346
4.042/ 262
3.858/ 217
3.345/ 168

FIG. 18A

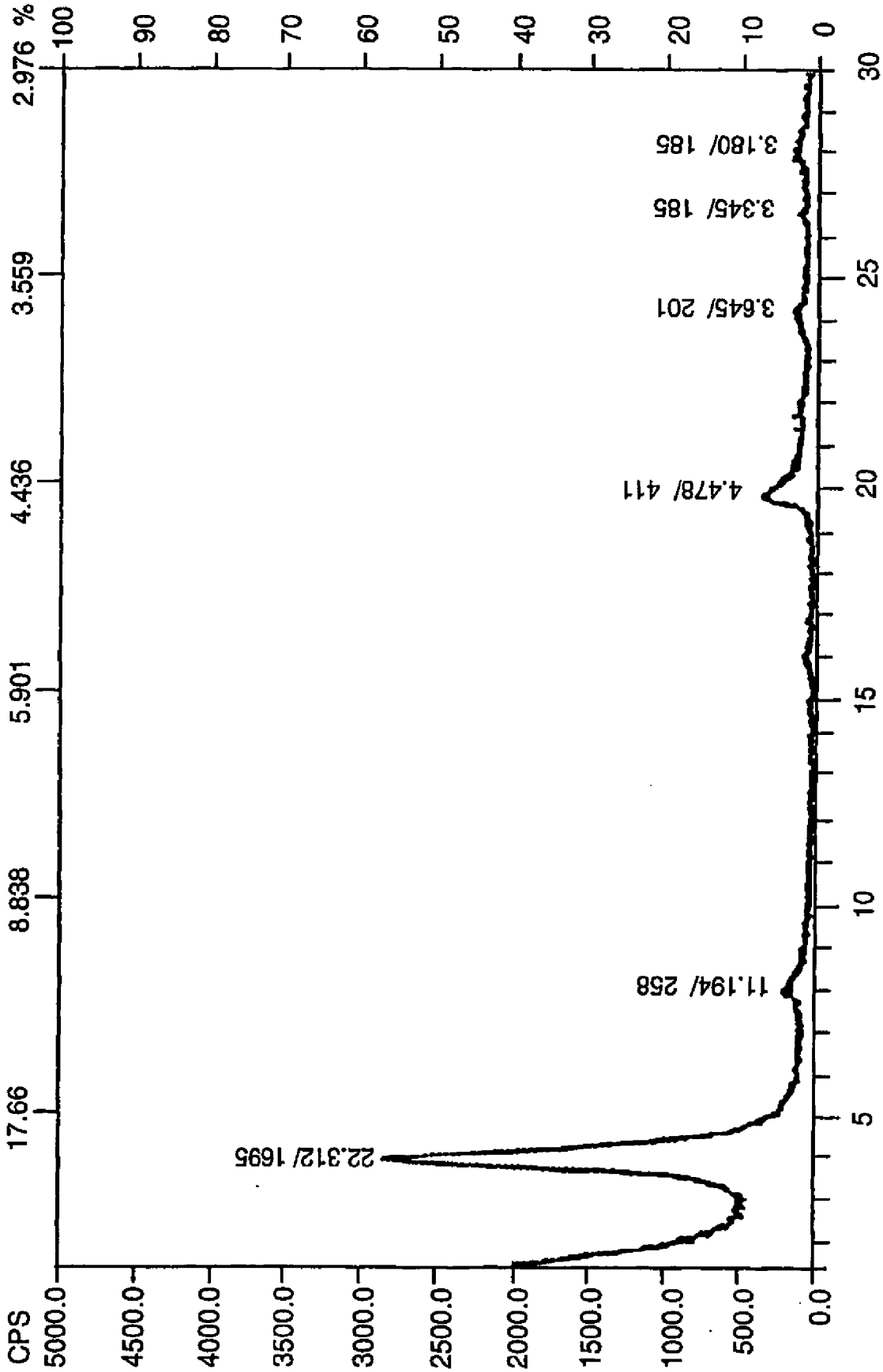
CPS
5000.0
4500.0
4000.0
3500.0
3000.0
2500.0
2000.0
1500.0
1000.0
500.0
0.0
17.66
8.838
5.901
4.436
3.559
2.976
%
100
90
80
70
60
50
40
30
20
10
0
5
10
15
20
25
30
22.312/ 1695
11.194/ 258
4.478/ 411
3.645/ 201
3.345/ 185
3.180/ 185

FIG. 18B

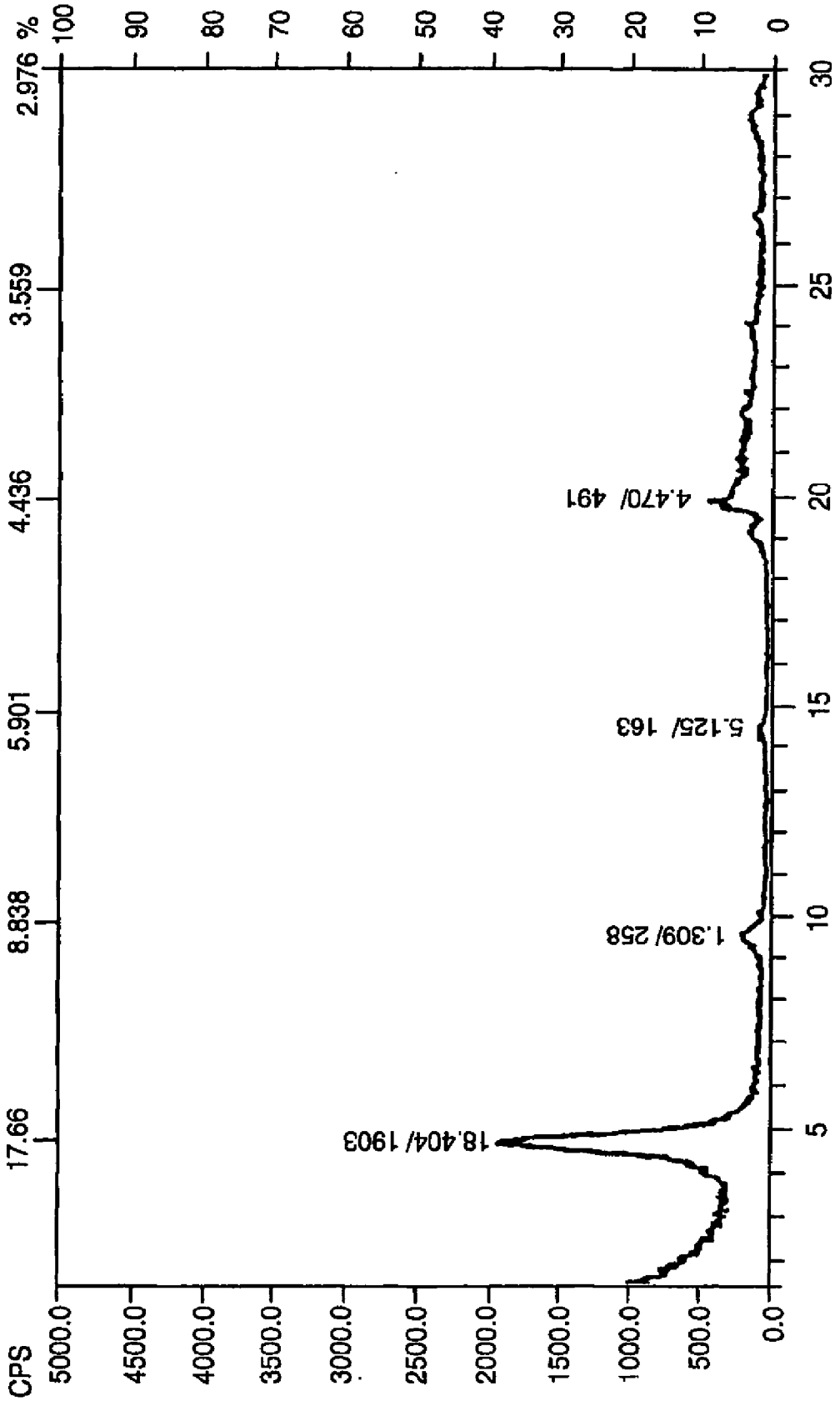
CPS
5000.0
4500.0
4000.0
3500.0
3000.0
2500.0
2000.0
1500.0
1000.0
500.0
0.0
%
100
90
80
70
60
50
40
30
20
10
0
2.976
3.559
4.436
5.901
8.838
17.66
18.404/ 1903
1.309/ 258
5.125/ 163
4.470/ 491
5
10
15
20
25
30

FIG. 18C

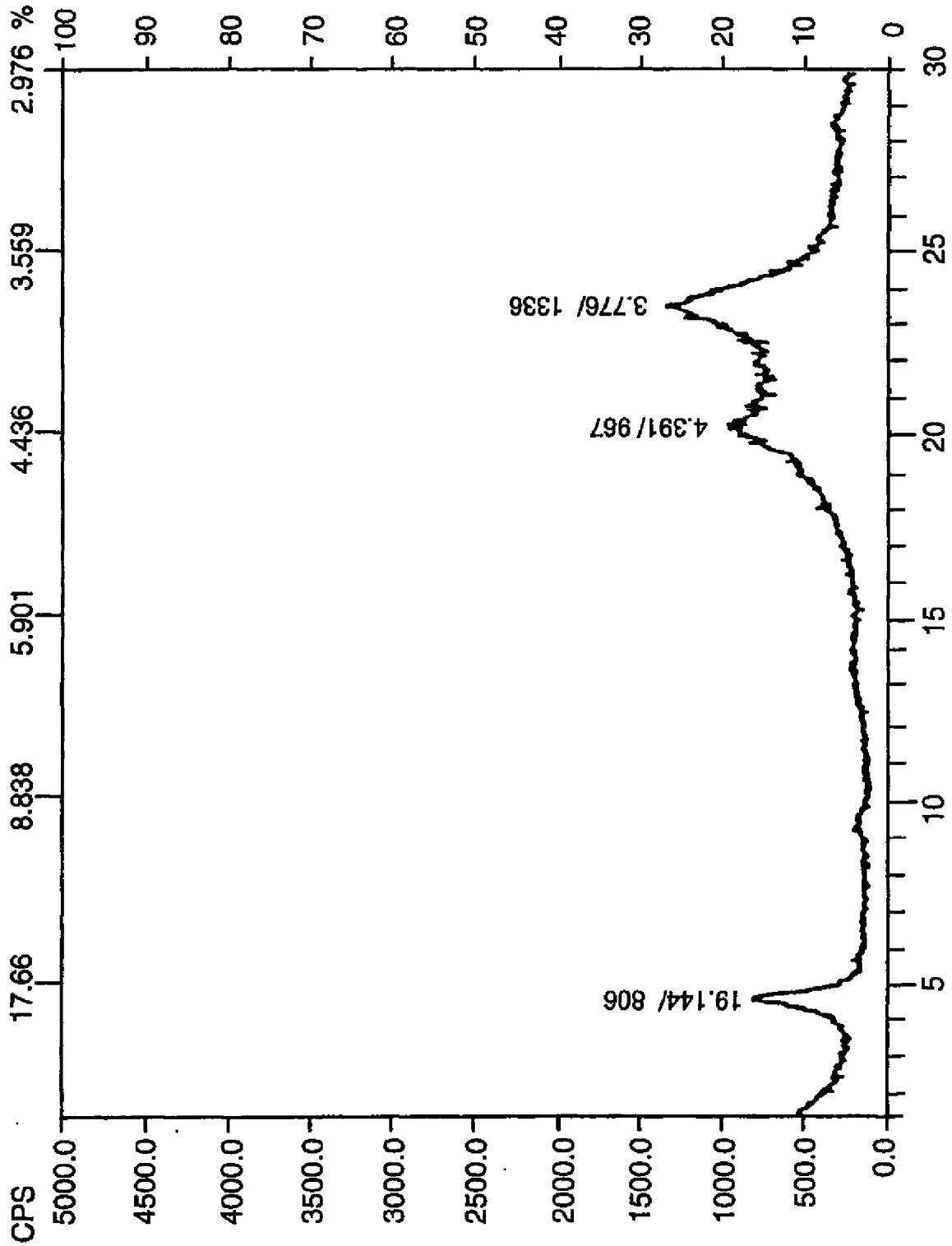
CPS
5000.0
4500.0
4000.0
3500.0
3000.0
2500.0
2000.0
1500.0
1000.0
500.0
0.0
17.66
8.838
5.901
4.436
3.559
2.976 %
100
90
80
70
60
50
40
30
20
10
0
5
10
15
20
25
30
19.144/ 806
4.391/ 967
3.776/ 1336

FIG. 19A

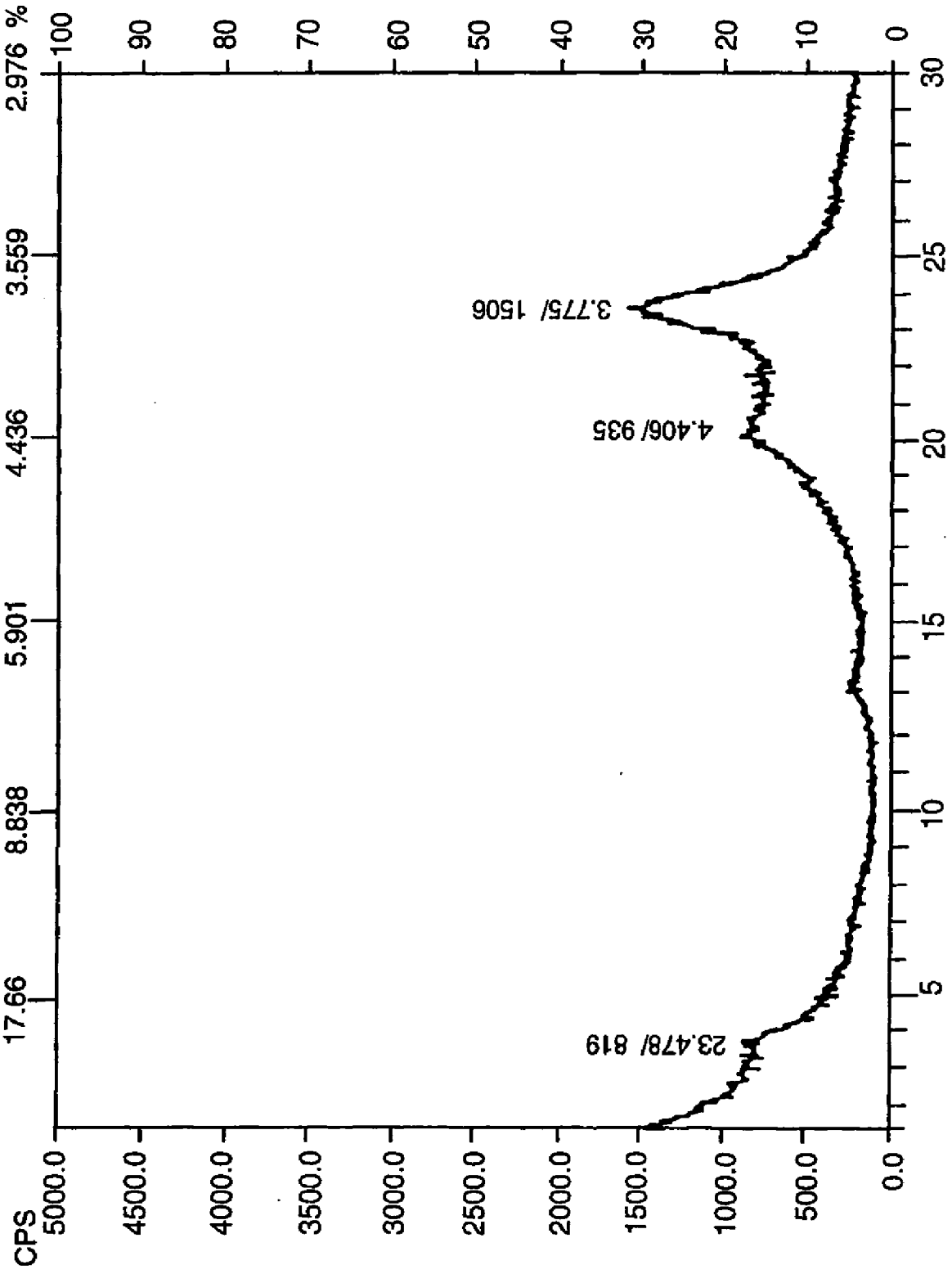
CPS
5000.0
4500.0
4000.0
3500.0
3000.0
2500.0
2000.0
1500.0
1000.0
500.0
0.0
17.66
8.838
5.901
4.436
3.559
2.976 %
100
90
80
70
60
50
40
30
20
10
0
30
25
20
15
10
5
23.478/ 819
4.406/ 935
3.775/ 1506

FIG. 19B

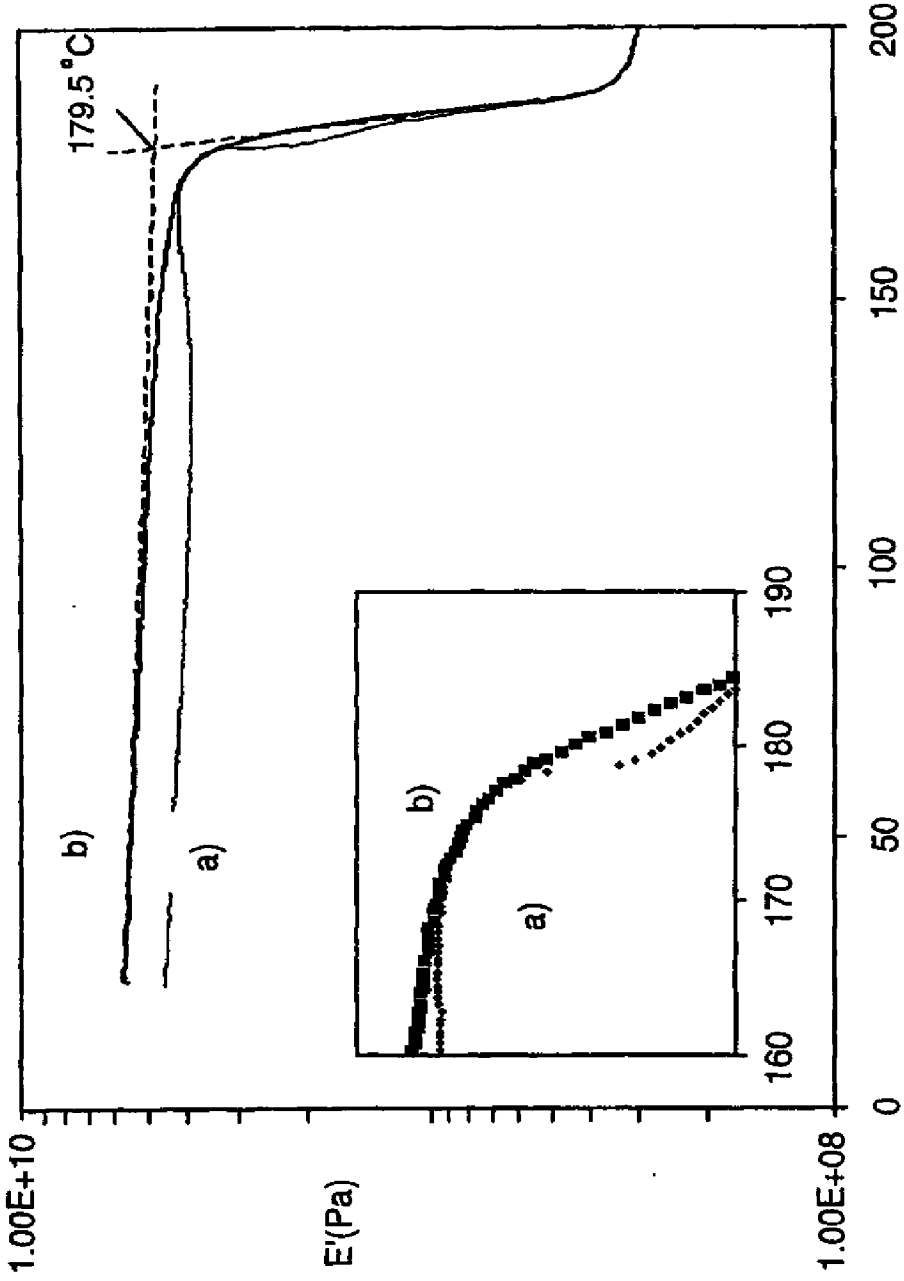

DMA CURVES FOR a) NEAT UDEL AND b) UDEL NANOCOMPOSITE

FIG. 20

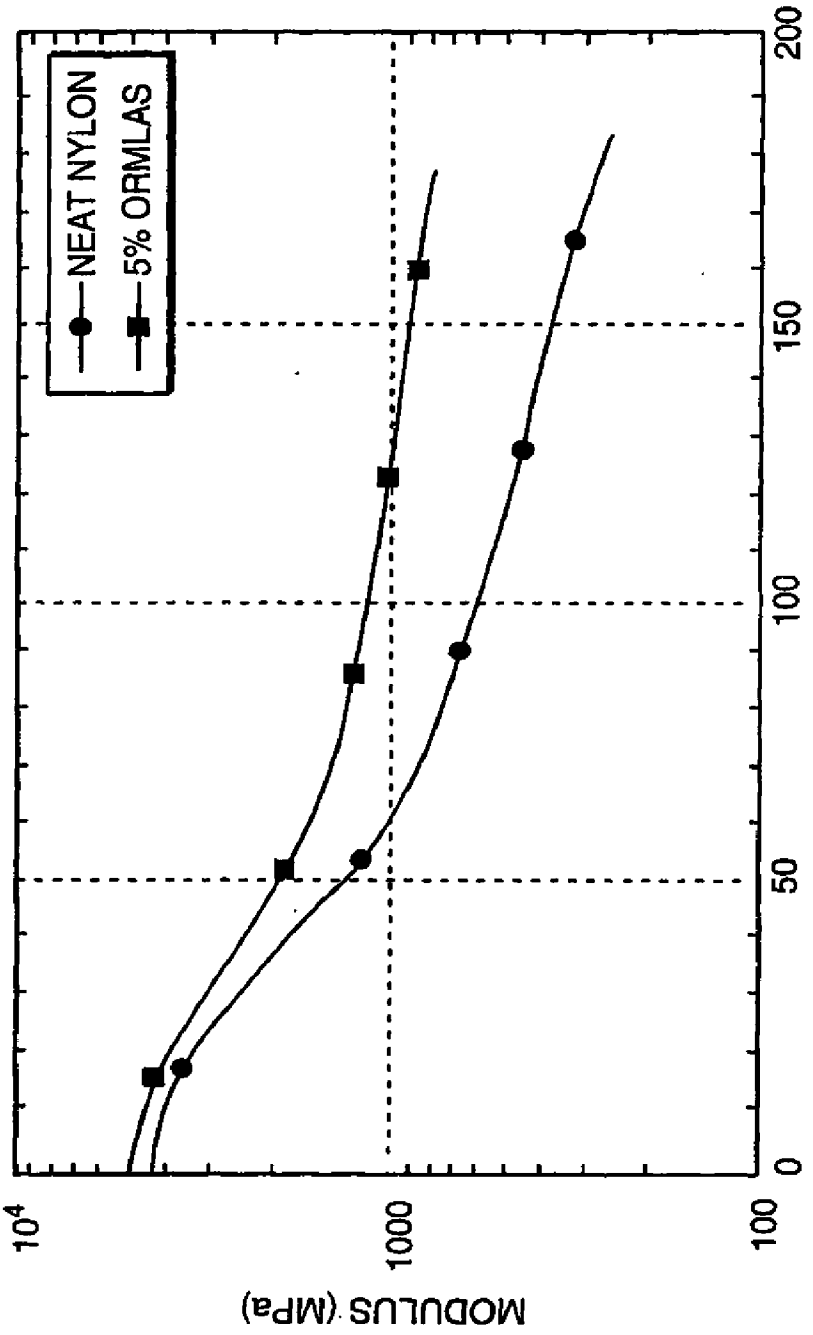
NEAT NYLON
5% ORMLAS
MODULUS (MPa)
10^4
1000
100
TEMPERATURE (DEG C)
0
50
100
150
200

FIG. 21

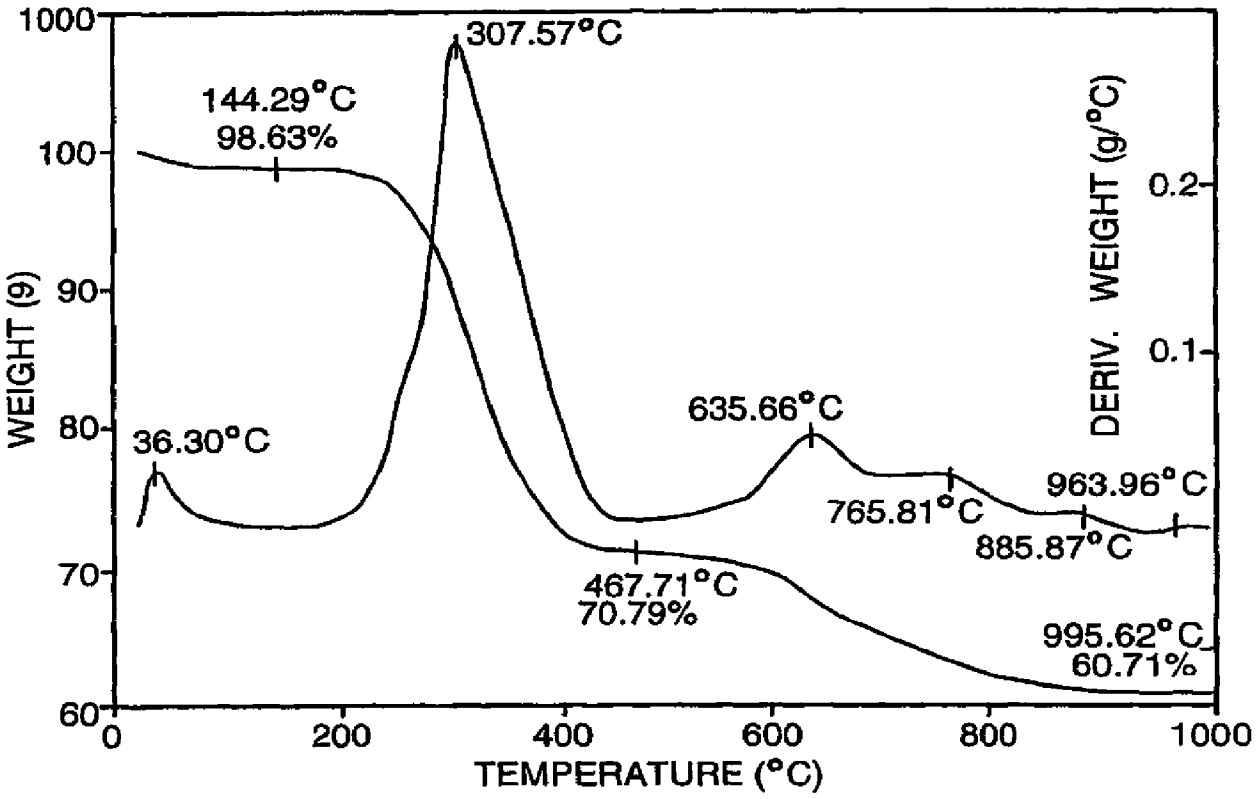

FIG. 22a

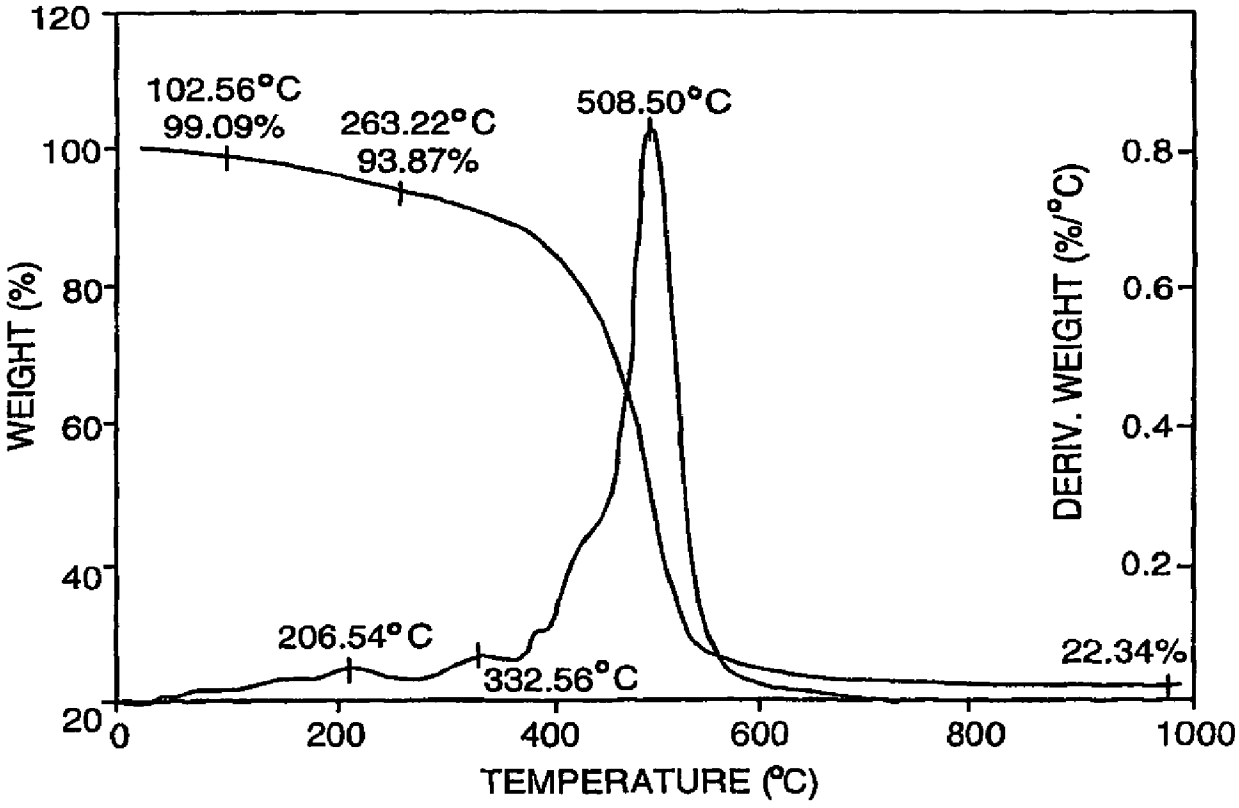

FIG. 22b

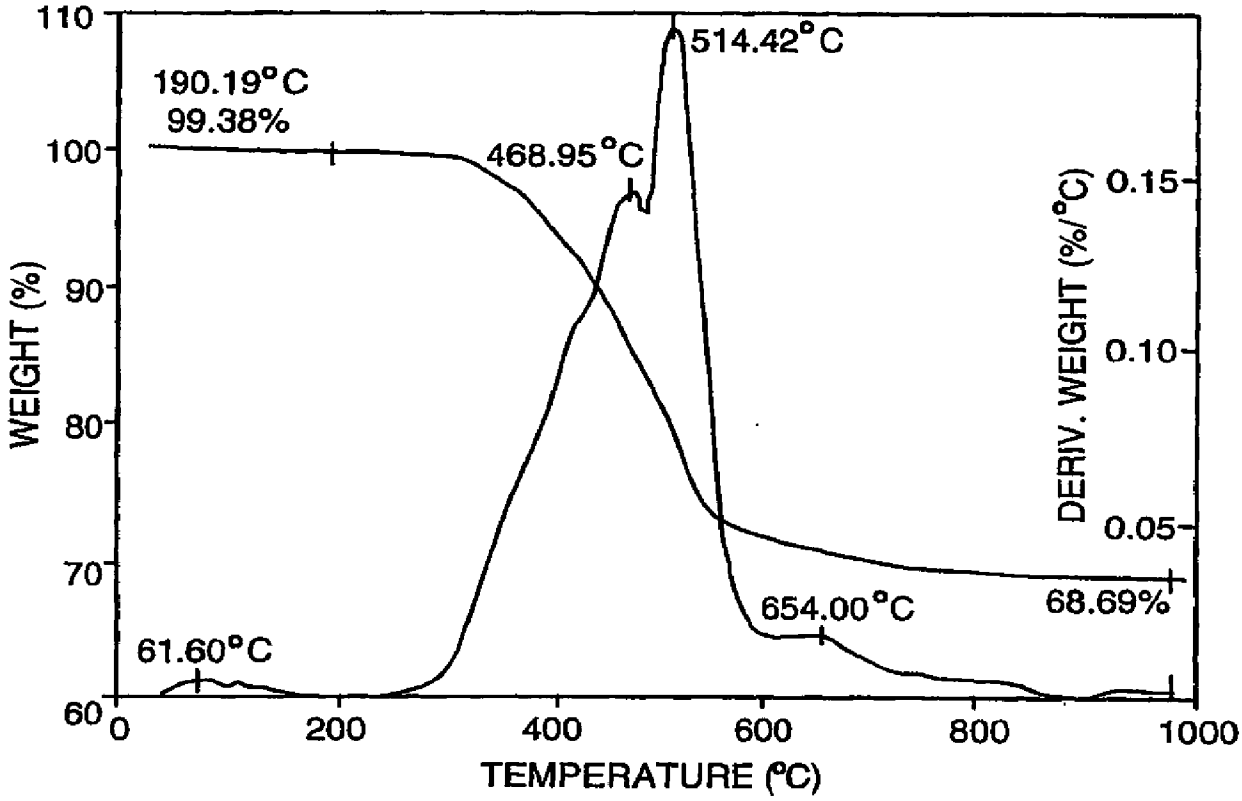

FIG. 22c

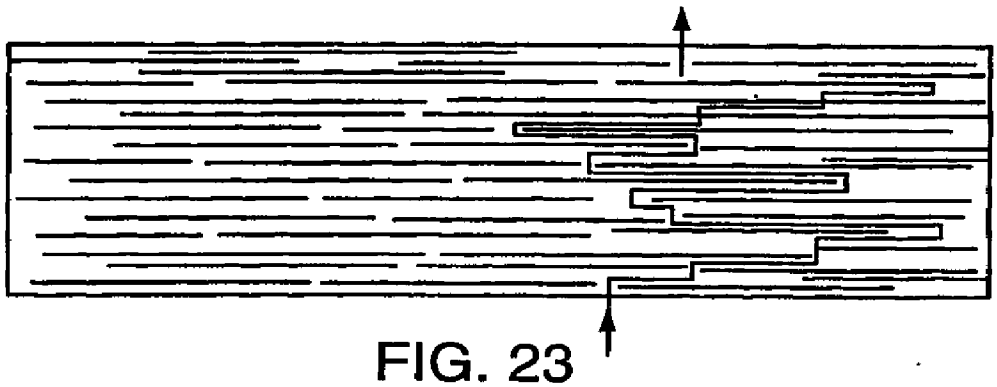

FIG. 23

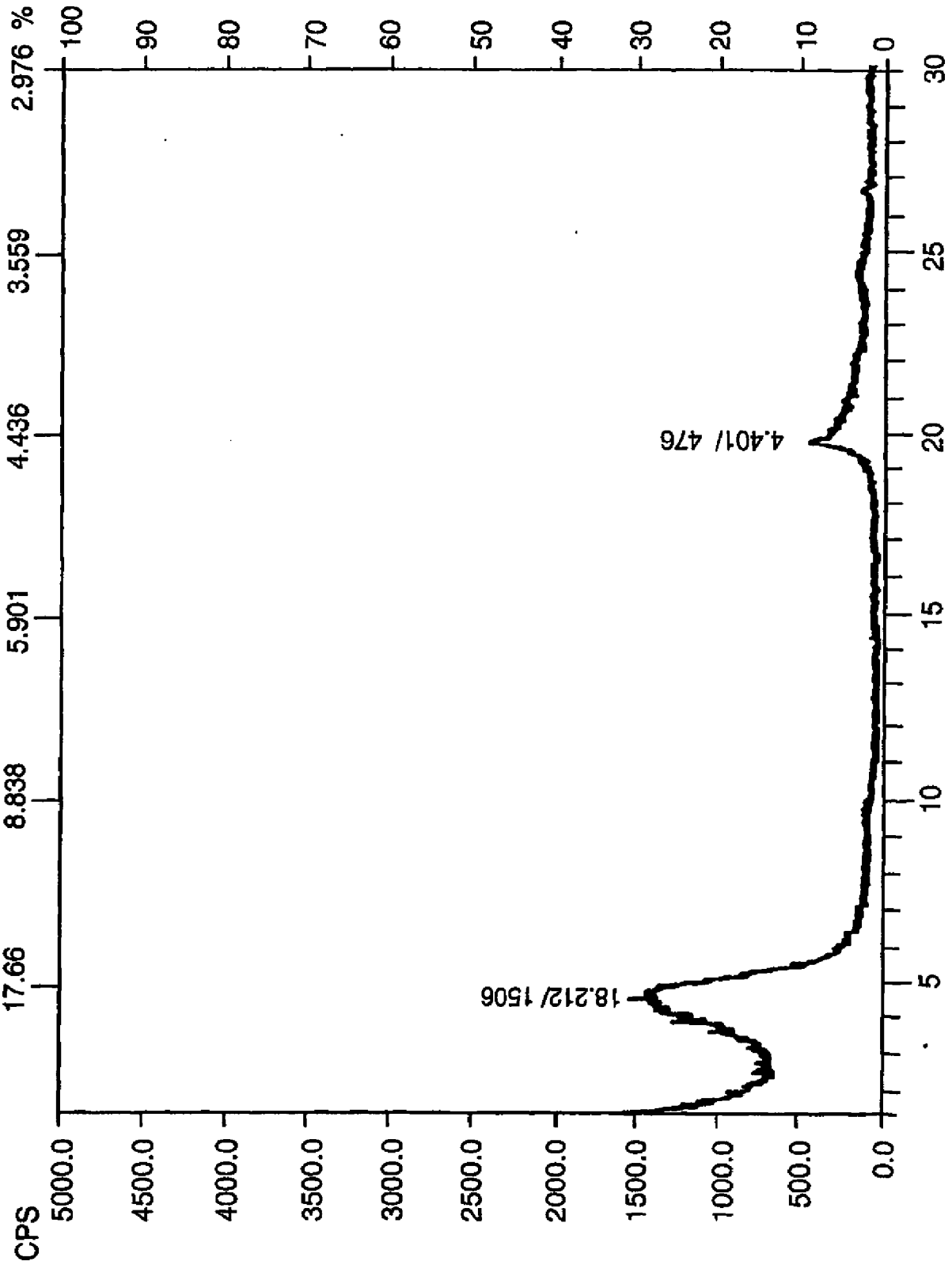
CPS
5000.0
4500.0
4000.0
3500.0
3000.0
2500.0
2000.0
1500.0
1000.0
500.0
0.0
17.66
8.838
5.901
4.436
3.559
2.976 %
100
90
80
70
60
50
40
30
20
10
0
5
10
15
20
25
30
18.212/ 1506
4.401/ 476

FIG. 24A

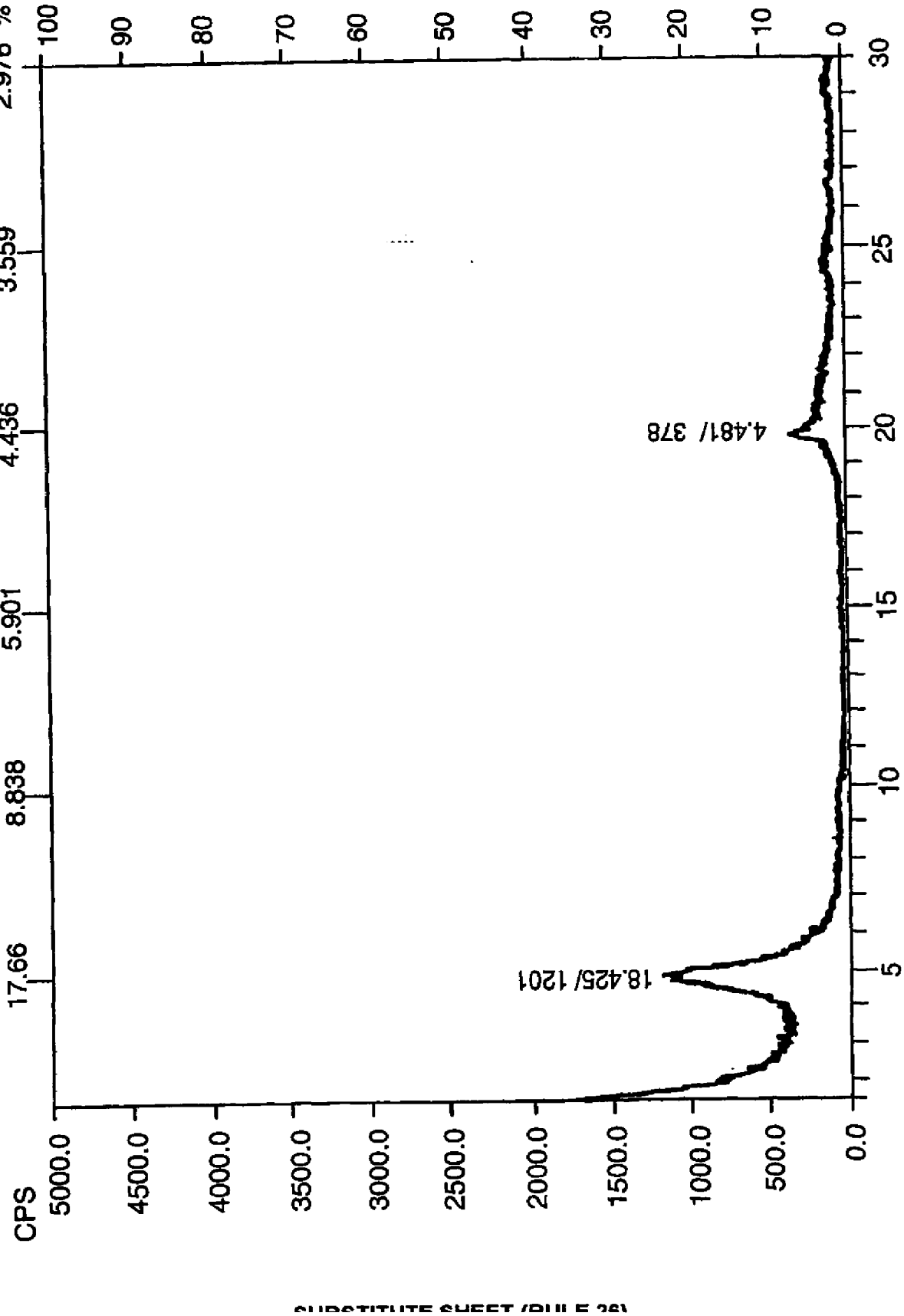
CPS
5000.0
4500.0
4000.0
3500.0
3000.0
2500.0
2000.0
1500.0
1000.0
500.0
0.0
17.66
8.838
5.901
4.436
3.559
2.976 %
100
90
80
70
60
50
40
30
20
10
0
5
10
15
20
25
30
18.425/ 1201
4.481/ 378

FIG. 24B

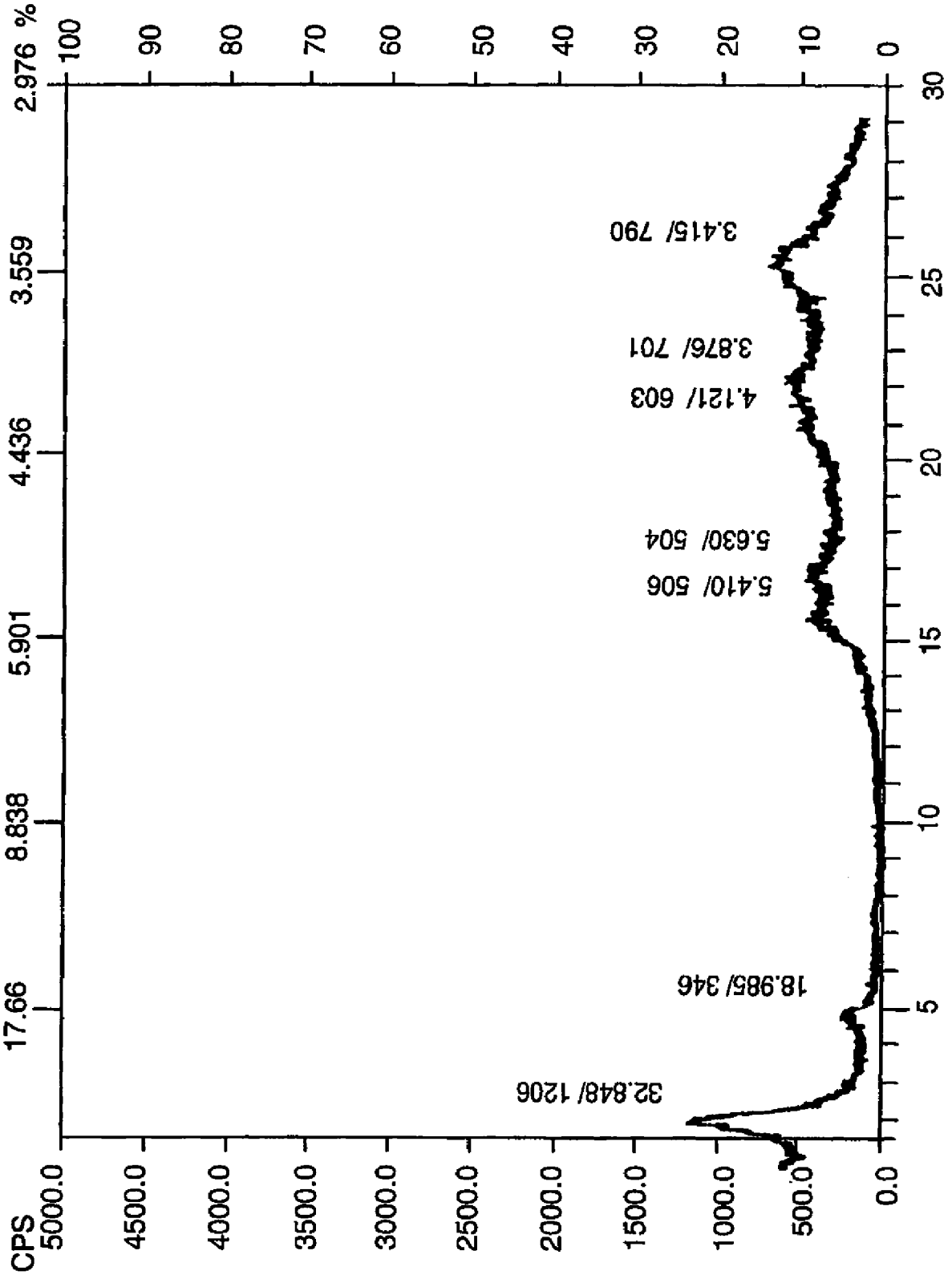
CPS
5000.0
4500.0
4000.0
3500.0
3000.0
2500.0
2000.0
1500.0
1000.0
500.0
0.0
17.66
8.838
5.901
4.436
3.559
2.976 %
100
90
80
70
60
50
40
30
20
10
0
30
25
20
15
10
5
32.848/ 1206
18.985/ 346
5.410/ 506
5.630/ 504
4.121/ 603
3.876/ 701
3.415/ 790

FIG. 25A

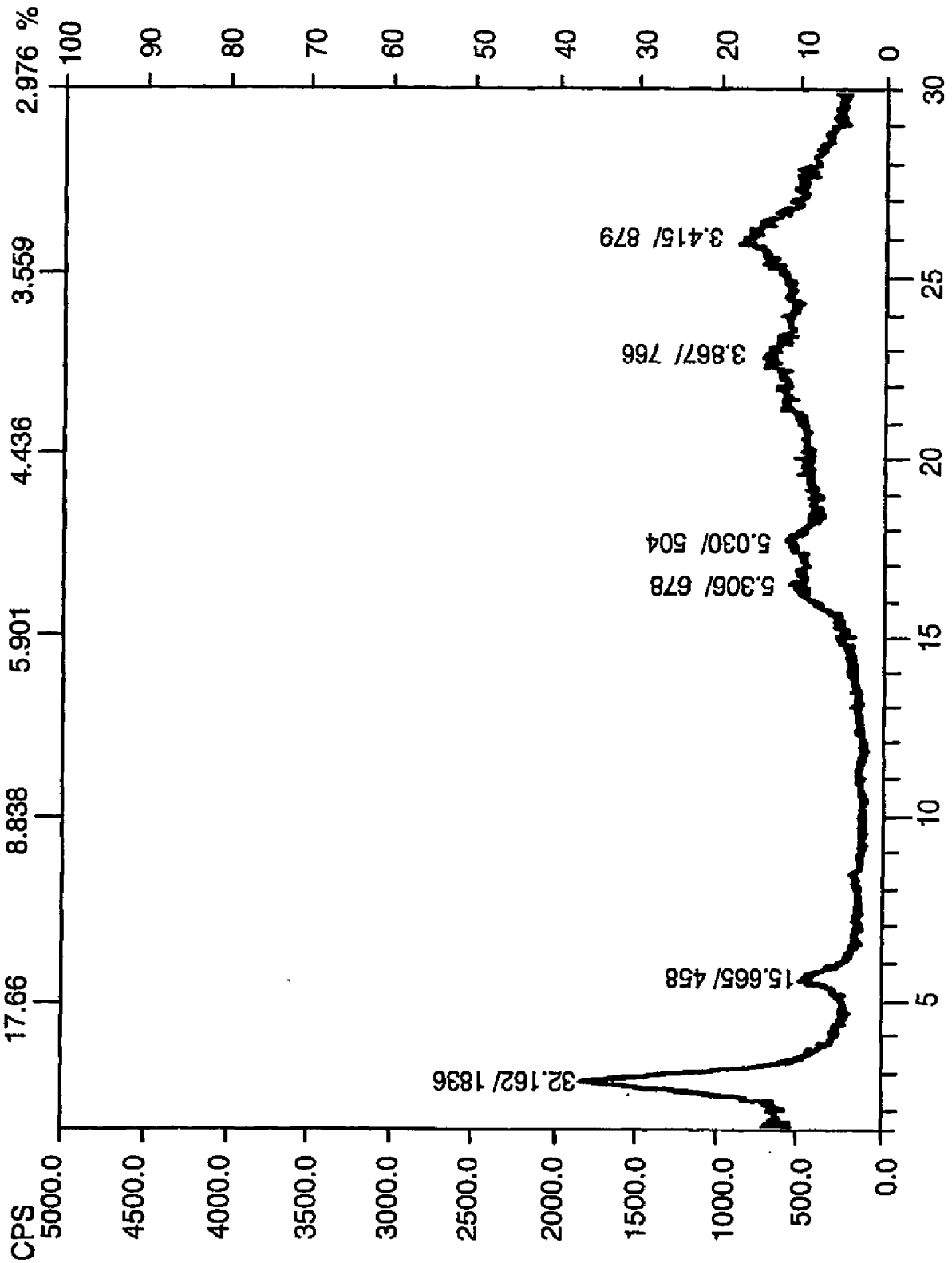
CPS
5000.0
4500.0
4000.0
3500.0
3000.0
2500.0
2000.0
1500.0
1000.0
500.0
0.0
17.66
8.838
5.901
4.436
3.559
2.976 %
100
90
80
70
60
50
40
30
20
10
0
30
25
20
15
10
5
32.162/ 1836
15.665/ 458
5.306/ 678
5.030/ 504
3.867/ 766
3.415/ 879

FIG. 25B

INTERNATIONAL SEARCH REPORT

International application No.
PCT/US00/16358

A. CLASSIFICATION OF SUBJECT MATTER

IPC(7) :B32B 15/02
US CL :428/402

According to International Patent Classification (IPC) or to both national classification and IPC

B. FIELDS SEARCHED

Minimum documentation searched (classification system followed by classification symbols)

U.S. : 428/402, 403, 404, 407

Documentation searched other than minimum documentation to the extent that such documents are included in the fields searched

Electronic data base consulted during the international search (name of data base and, where practicable, search terms used)

C. DOCUMENTS CONSIDERED TO BE RELEVANT

Category*	Citation of document, with indication, where appropriate, of the relevant passages	Relevant to claim No.
X --- Y	US 5,707,439 A (TAKEKOSHI et al.) 13 January 1998, see entire document.	1-7,21-26,3 2,55-56 --- 8-20,33-35,49-54,57-63
X --- Y	US 5,807,629 A (ELSPASS et al.) 15 September 1998, see entire document.	1-7,21-26,32,55-56 --- 8-20,33-35,49-54,57-63

☐ Further documents are listed in the continuation of Box C. ☐ See patent family annex.

*	Special categories of cited documents:	"T"	later document published after the international filing date or priority date and not in conflict with the application but cited to understand the principle or theory underlying the invention
"A"	document defining the general state of the art which is not considered to be of particular relevance	"X"	document of particular relevance; the claimed invention cannot be considered novel or cannot be considered to involve an inventive step when the document is taken alone
"E"	earlier document published on or after the international filing date	"Y"	document of particular relevance; the claimed invention cannot be considered to involve an inventive step when the document is combined with one or more other such documents, such combination being obvious to a person skilled in the art
"L"	document which may throw doubts on priority claim(s) or which is cited to establish the publication date of another citation or other special reason (as specified)	"&"	document member of the same patent family
"O"	document referring to an oral disclosure, use, exhibition or other means		
"P"	document published prior to the international filing date but later than the priority date claimed		

Date of the actual completion of the international search	Date of mailing of the international search report
14 JULY 2000	28 AUG 2000

Name and mailing address of the ISA/US	Authorized officer
Commissioner of Patents and Trademarks Box PCT Washington, D.C. 20231	ELIZABETH EVANS